Approximation and Convergence of the Intrinsic Volume *

Herbert Edelsbrunner† and Florian Pausinger†

October 27, 2014

Abstract

We introduce a modification of the classic notion of intrinsic volume using persistence moments of height functions. Evaluating the modified first intrinsic volume on digital approximations of a compact body with smoothly embedded boundary in $\mathbb{R}^n$, we prove convergence to the first intrinsic volume of the body as the resolution of the approximation improves. We have weaker results for the other modified intrinsic volumes, proving they converge to the corresponding intrinsic volumes of the n-dimensional unit ball.

Keywords: Persistent homology; intrinsic volume; Crofton formula; digital image processing; distorted normals.

MSC2010: 65D18, 53C65, 28A75, 55N99, 53A05.

Contents

*This research is partially supported by the Toposys project FP7-ICT-318493-STREP, and by ESF under the ACAT Research Network Programme.

†IST Austria (Institute of Science and Technology Austria), Klosterneuburg, Austria.

1 Introduction

Let $\mathbb{M}$ be a compact body in $\mathbb{R}^3$ whose boundary, $\partial\mathbb{M}$, is a smoothly embedded 2-manifold, and let t be a possibly small but positive real parameter. Letting $\#(\mathbb{M} \cap t\mathbb{Z}^3)$ be the number of points of the dilated integer grid in $\mathbb{M}$, it is well known that $t^3\#(\mathbb{M} \cap t\mathbb{Z}^3)$ converges to $\mathrm{Vol}(\mathbb{M})$ as t goes to zero. The central question of the classic lattice point theory, as founded by E. Landau and others in the first decades of the 20th century, is to estimate the *lattice discrepancy*, which is defined as $t^3\#(\mathbb{M} \cap t\mathbb{Z}^3) - \mathrm{Vol}(\mathbb{M})$; see the recent survey [18] for more details. Since the lattice discrepancy vanishes as t goes to zero, we may approximate $\mathbb{M}$ with $\#(\mathbb{M} \cap t\mathbb{Z}^3)$ cubes of edge length t whose centers are in $\mathbb{M} \cap t\mathbb{Z}^3$, such that the volume is preserved asymptotically, as t goes to zero. It would be nice to also preserve the other *intrinsic volumes* of $\mathbb{M}$, namely the surface area, the total mean curvature, and the total Gaussian curvature, by means of the above approximation with cubes. However, a straightforward construction only yields the right volume and Gaussian curvature, while the surface area and the mean curvature of the approximation can significantly differ from the values of $\mathbb{M}$ as the following example shows.

Motivating example. Let $\mathbb{M} = \mathbb{B}^3$ be the unit ball in $\mathbb{R}^3$. The *resolution t digital approximation* of $\mathbb{B}^3$, denoted as $\mathbb{B}^3_t$, is the union of axes-aligned cubes of edge length t whose centers are of the form (tx, ty, tz), with $(x, y, z) \in \mathbb{Z}^3$ and $t\sqrt{x^2 + y^2 + z^2} \leq 1$. There are $\#(\mathbb{B}^3 \cap t\mathbb{Z}^3) = \mathrm{Vol}(\mathbb{B}^3)/t^3 + o(1/t^3)$ such cubes, each with volume t^3. Hence,

$$\lim_{t\to 0} \mathrm{Vol}(\mathbb{B}^3_t) = \lim_{t\to 0} t^3\#(\mathbb{B}^3 \cap t\mathbb{Z}^3) = \mathrm{Vol}(\mathbb{B}^3). \tag{1}$$

As for the surface area, we note that if we look from either end of each of the three coordinate axes, we see every square face in the boundary of $\mathbb{B}^3_t$ exactly once. From each of the six directions, we see $\#(\mathbb{B}^2 \cap t\mathbb{Z}^2)$ faces, each of area t^2. As t goes to zero, the total area of these faces converges to the area of the unit disk, which implies

$$\lim_{t\to 0} \mathrm{Area}(\mathbb{B}^3_t) = 6 \lim_{t\to 0} t^2\#(\mathbb{B}^2 \cap t\mathbb{Z}^2) = 6\mathrm{Area}(\mathbb{B}^2), \tag{2}$$

which is 6π. In contrast, the surface area of the boundary of the unit ball is 4π. Moving on to the total mean curvature, we use a discrete formulation according to which the contribution of a convex edge is $\pi/4$ times its length, and that of a reflex edge is $-\pi/4$ times its length. Again looking at $\mathbb{B}^3_t$ from either end of the three coordinate axes, we record the contributions of all convex and reflex edges in the boundary of visible square faces. These edges are organized in curves delimiting steps, and we can pair up the reflex with the convex edges, effectively cancelling their contributions to the total mean curvature. This leaves the convex edges of the last step (the silhouette) unpaired. The total length of these edges is $4t\#(\mathbb{B}^1 \cap t\mathbb{Z})$, which converges to four times the length of $\mathbb{B}^1$. We get the total mean curvature by

multiplying with 6 for the number of directions, with $\frac{1}{2}$ because each convex and reflex edge is accounted for twice, and $\frac{\pi}{4}$ for half the dihedral angle at the convex edges. Hence,

$$\lim_{t\to 0} \text{Mean}(\mathbb{B}^3_t) = \tfrac{6\pi}{8} \lim_{t\to 0} 4t\#(\mathbb{B}^1 \cap t\mathbb{Z}) = 3\pi \text{Length}(\mathbb{B}^1), \tag{3}$$

which is 6π. In contrast, the total mean curvature of the boundary of the unit ball is 4π. Finally, we compute the total Gaussian curvature of $\mathbb{B}^3_t$ as the sum of angle defects over all boundary vertices. This sum depends on the topological type of $\partial\mathbb{B}^3_t$ but not on its shape. The type is that of the sphere, for which the sum of angle defects is 4π. In other words, $\text{Gauss}(\mathbb{B}^3_t) = 4\pi = \text{Gauss}(\mathbb{B}^3)$ independent of t.

Results and prior work. The first main result of this paper modifies the notion of intrinsic volume to overcome the lack of convergence demonstrated in our motivating example. We use special cases of the Crofton and the Blaschke-Petkantschin Formulas to write the $(n-k)$-th intrinsic volume as an integral over k-planes, which we rewrite in terms of level sets of height functions. Using methods from computational topology, we summarize the contributions of a height function by the moment of its persistence diagram, but one that ignores small persistence contributions. Quantifying small as anything with persistence at most $t\sqrt{n}$, we prove that

$$\lim_{t\to 0} V_{n-k}(\mathbb{B}^n_t, t\sqrt{n}) = V_{n-k}(\mathbb{B}^n), \tag{4}$$

for all $0 \leq k < n$, in which $V_{n-k}(\mathbb{B}^n)$ is the $(n-k)$-th intrinsic volume of the n-dimensional unit ball, and $V_{n-k}(\mathbb{B}^n_t, t\sqrt{n})$ is the modified $(n-k)$-th intrinsic volume of the resolution t digitization of $\mathbb{B}^n$. See the Convergence Theorem for Balls for a more detailed statement of this result. For values of $n-k$ for which $V_{n-k}(\mathbb{B}^n_t)$ does not converge to $V_{n-k}(\mathbb{B}^n)$, this implies that the difference is primarily due to features of $\mathbb{B}^n_t$ that have small persistence under height functions.

Beyond providing structural insights, the convergence results imply multigrid convergent digital algorithms. In contrast to our approach, a *local digital algorithm* counts local configurations in a small observation window that moves over the digital image. Studying this special class of algorithms, Svane [22] proves that multigrid convergence cannot be achieved for the intrinsic volumes of convex bodies other than for V_n, which is the n-dimensional volume. The local algorithms are simple and thus often preferred over the most common type of non-local digital algorithms, which construct polytopes to approximate geometric sets and estimate their intrinsic volumes; see [15] and the references therein. As an example, we mention the probabilistic algorithm that estimates the intrinsic volumes of a convex body from the convex hull of randomly chosen points inside the body. For convex bodies whose boundaries have positive reach, it can be shown that the expected value of the $(n-k)$-th intrinsic volume of the convex hull converges to that of the convex body, for $0 \leq k \leq n$, as the number of points goes to infinity; see [4, 13].

The technical smoothness condition is not needed if $n - k = 1$. For non-convex bodies, the problem is more difficult. We mention a preprint of Meschenmoser, Spodarev [16] proposing a multigrid convergent algorithm to estimate all intrinsic volumes of a finite union of compact sets with positive reach. However, due to difficulties in constructing the required polytopes, the algorithm has not been implemented beyond the 2-dimensional case.

Our second result implies a multigrid convergent digital algorithm for computing the first intrinsic volume of not necessarily convex sets. This includes the length of boundary curves in $\mathbb{R}^2$ and the total mean curvature of boundary surfaces in $\mathbb{R}^3$. Specifically, we prove that

$$\lim_{t \to 0} V_1(\mathbb{M}_t, t\sqrt{n}) = V_1(\mathbb{M}), \tag{5}$$

in which $\mathbb{M}$ is a compact set in $\mathbb{R}^n$ whose boundary is a smoothly embedded $(n-1)$-manifold. See the Convergence Theorem for Solid Bodies for a more detailed statement of this result. An important ingredient in the proof of (5) is the explicit construction of a fibration of the symmetric difference of $\mathbb{M}$ and $\mathbb{M}_t$. Among other things, it implies that for sufficiently small t, $\mathbb{M}$ and $\mathbb{M}_t$ have the same homotopy type, which is new. A version of the modified intrinsic volume in (5) was used in [9] to estimate the length of tube-like shapes in $\mathbb{R}^3$. Without proving convergence, this paper implemented the digital algorithm thus illustrating the practical potential of our result. Indeed the implied digital algorithm is readily implemented as it reduces to the computation of persistence diagrams of height functions – a task that has fast software due to the focused attention it received within computational topology; see [8].

Outline. Section 2 presents the background on digital algorithms, intrinsic volume, and persistent homology. Section 3 introduces the modification of the intrinsic volume. Section 4 proves convergence for the n-dimensional unit ball. Section 5 introduces the new concept of the distorted normal bundle of the sphere, which is then extended to more general solid bodies in Section 6. Section 7 proves convergence of the modified first intrinsic volume for compact bodies with smoothly embedded boundaries in $\mathbb{R}^n$. Section 8 comments on the algorithms implied by our results and states open questions.

2 Background

Beyond the material presented in this section, we refer to Bonnesen, Fenchel [3] and Schneider [20] for further background on intrinsic volumes, to Morvan [17] for various generalizations of the convex theory, and to Schneider, Weil [21] for a thorough introduction to integral geometry. We refer to Edelsbrunner, Harer [8] for further background on persistent homology.

Digital algorithms. Throughout this paper, $\mathbb{Z}^n$ denotes the integer lattice in $\mathbb{R}^n$. For $t > 0$, we call $t\mathbb{Z}^n$ the *scaled integer lattice*, and t its *resolution*. Given a set $\mathbb{M} \subseteq \mathbb{R}^n$, the *binary* or *hit-or-miss digitization at resolution t* is $\mathbb{M} \cap t\mathbb{Z}^n$, the set of scaled integer points contained in the set; see [19]. We write $\mathbb{M}_t$ for the union of the axes-aligned n-cubes with edge length t centered at the points in $\mathbb{M} \cap t\mathbb{Z}^n$. Let $\mathcal{S}$ be a class of subsets of $\mathbb{R}^n$, and let $\mu \colon \mathcal{S} \to \mathbb{R}$ be some function. We are interested in estimating this function using digitizations of the subsets. Following [15], we define a *digital algorithm* of μ as a 1-parameter family of real-valued functions on the power sets of the scaled integer lattices:

$$\mu_t \colon 2^{t\mathbb{Z}^n} \to \mathbb{R}, \tag{6}$$

for every $t > 0$. Call $\mu_t(\mathbb{M}_t)$ the *resolution t digital estimator* for $\mu(\mathbb{M})$. The question arises how the digital algorithm should relate to the function. Obviously, many different sets may have the same digitization, so $\mu_t(\mathbb{M}_t)$ will usually not give the correct value. Is it possible to obtain a geometric functional from the digitization, at least asymptotically, as t tends to 0? The answer depends on the class of sets we consider. To make the question more precise, we call a digital algorithm *multigrid convergent* for $\mu \colon \mathcal{S} \to \mathbb{R}$ if $\lim_{t \to 0} \mu_t(\mathbb{M}_t) = \mu(\mathbb{M})$, for every $\mathbb{M} \in \mathcal{S}$. As example we mention the volume functional in $\mathbb{R}^n$, $\mathrm{Vol}_n \colon \mathcal{K}^n \to \mathbb{R}$, defined by mapping a convex set to its n-dimensional volume. The digital algorithm that maps every finite subset of $t\mathbb{Z}^n$ to t^n times its cardinality is multigrid convergent for Vol_n.

Intrinsic volumes. Let $\mathbb{K}$ be a convex body in $\mathbb{R}^n$, and write $\mathbb{K}_r = \mathbb{K} + r\mathbb{B}^n$ for the *parallel body* with *offset* $r \geq 0$. The *Steiner polynomial* of $\mathbb{K}$ gives the volume of $\mathbb{K}_r$ as a function of r. It is a degree-n polynomial whose coefficients are given in two common notations:

$$\mathrm{Vol}_n(\mathbb{K}_r) = \sum_{k=0}^{n} \binom{n}{k} W_k(\mathbb{K})\, r^k = \sum_{k=0}^{n} b_k V_{n-k}(\mathbb{K})\, r^k. \tag{7}$$

In the classical literature, the W_k are called the *quermassintegrals*, and the V_k, which came into use later, are referred to as the *intrinsic volumes* of $\mathbb{K}$. The *volume*, V_n, the *surface area*, $2V_{n-1}$, and the *Euler characteristic*, $V_0 = \chi$, are often of special interest. For further details and a proof of the Steiner formula, we refer to [20, Chapter 4]. The intrinsic volumes can be characterized by their properties, namely that they are additive, motion invariant, and continuous. Their importance is underlined by Hadwiger's Characterization Theorem, which states that any additive, motion invariant, and continuous function on $\mathcal{K}^n$ is a linear combination of the intrinsic volumes. A proof of the Characterization Theorem in three dimensions was given in [11], and in arbitrary dimensions in [12]; see also [20].

The Crofton Formula provides integral representations for the coefficients in the Steiner polynomial and sheds light on the old German name of quermassintegrals. We use a special case to connect the theories of intrinsic volumes and persistent homology. Writing λ_n for the Lebesgue measure on $\mathbb{R}^n$, we let $b_n = \lambda_n(\mathbb{B}^n)$

be the n-dimensional volume of the unit ball, and writing σ_{n-1} for the spherical Lebesgue measure on $\mathbb{S}^{n-1}$, we get $s_n = \sigma_{n-1}(\mathbb{S}^{n-1}) = nb_n$ for the $(n-1)$-dimensional area of the unit sphere. When we integrate with respect to a Lebesgue measure, we simplify notation by writing $\mathrm{d}y$ for $\lambda_n(\mathrm{d}y)$. Moreover, we write $\mathcal{L}^n_k \subseteq \mathcal{E}^n_k$ for the sets of k-dimensional linear and affine subspaces of $\mathbb{R}^n$. These sets are also known as the *Grassmannian* and *affine Grassmannian*. The latter consists of all k-planes in $\mathbb{R}^n$, while the former contains only those that pass through the origin. Assuming $j \leq k$, we write $\mathcal{L}^E_j \subseteq \mathcal{E}^E_j$ for the sets of linear and affine j-planes contained in $E \in \mathcal{E}^n_k$. There exists a unique rotation invariant Haar measure, ν_k, on $\mathcal{L}^n_k$, normalized by $\nu_k(\mathcal{L}^n_k) = 1$, and a unique motion invariant Haar measure, μ_k on $\mathcal{E}^n_k$, normalized so that $\mu_k(\{E \in \mathcal{E}^n_k \mid E \cap \mathbb{B}^n \neq \emptyset\}) = b_{n-k}$. When we integrate, we write $\mathrm{d}L$ and $\mathrm{d}E$ instead of $\nu_k(\mathrm{d}L)$ and $\mu_k(\mathrm{d}E)$. See [21, Chapter 13] for further details on the construction of the Haar measures. The classical Crofton Formula relates the intrinsic volumes of the k-dimensional sections to the intrinsic volume of the original set; see [14, Theorem 2.4]. Throughout this paper, we use the special case

$$V_{n-k}(\mathbb{K}) = c_{k,n} \cdot \int_{E \in \mathcal{E}^n_k} \chi(\mathbb{K} \cap E)\, \mathrm{d}E \tag{8}$$

$$= c_{k,n} \cdot \int_{L \in \mathcal{L}^n_k} \int_{y \in L^\perp} \chi\left(\mathbb{K} \cap (L + y)\right)\, \mathrm{d}y\, \mathrm{d}L \tag{9}$$

for $0 \leq k \leq n$, where $\mathbb{K} \in \mathcal{K}^n$ is a convex body in $\mathbb{R}^n$, $\chi(\mathbb{K} \cap E)$ is the Euler characteristic of the intersection, and $c_{k,n} = \binom{n}{k} \frac{b_n}{b_k b_{n-k}}$. A proof of the second line can be found in [21, Theorem 13.2.12]. Intuitively, it follows from the fact that every $E \in \mathcal{E}^n_k$ has a unique parallel $L \in \mathcal{L}^n_k$, and L has a unique *orthogonal complement* defined as the $(n-k)$-plane $L^\perp \in \mathcal{L}^n_{n-k}$ that forms a right angle with L. Writing $E = L + y$ with $y \in L^\perp$, we get the expression of the intrinsic volume as the double integral stated in (9).

The theory of convex bodies has important generalizations to more general classes of sets. Especially (7), (8), (9) have been extended to the class of *polyconvex sets* [20], and to the class of *tubes*, yielding the famous Tube Formula of Weyl [23]. Furthermore, Federer [10] developed an extensive theory of curvature measures for sets of *positive reach* and proved the Crofton Formula for this class of sets; see [10] and [20, Notes for Section 4.4].

Persistent homology. We begin by introducing persistent homology for height functions, generalizing to the more abstract setting of towers of vector spaces later. Given a direction $u \in \mathbb{S}^{n-1}$, the *height function* on $\mathbb{M} \subseteq \mathbb{R}^n$ in direction u is defined by mapping x to $f(x) = \langle x, u \rangle$. The *level set* of f at $r \in \mathbb{R}$, defined as $f^{-1}(r)$, is the intersection of $\mathbb{M}$ with the $(n-1)$-plane of points $\langle x, u \rangle = r$. Our interest in persistent homology is motivated by the structural insight it offers into the family of level sets. It is constructed using *sublevel sets*, $\mathbb{M}_r = f^{-1}(-\infty, r]$, and *superlevel sets*, $\mathbb{M}^r = f^{-1}[r, \infty)$. Assume finitely many *homological critical values*, v_1 to v_m, defined such that for any two values r and r' contained in one of the $m+1$

open intervals, the homology groups of $\mathbb{M}_r$ and $\mathbb{M}_{r'}$ are isomorphic and so are the relative homology groups of the pairs $(\mathbb{M}, \mathbb{M}^r)$ and $(\mathbb{M}, \mathbb{M}^{r'})$. Choose interleaving homological regular values such that $r_0 < v_1 < r_1 < \ldots < v_m < r_m$, and write $\mathsf{H}_i = H(\mathbb{M}_{r_i})$ and $\mathsf{H}_{2m-i} = H(\mathbb{M}, \mathbb{M}^{r_i})$ for the corresponding homology groups. Here, H is the homology functor that maps a space or a pair of spaces to the direct sum of the homology groups in all dimensions. Assuming field coefficients in the construction of homology, the H_i are vector spaces connected by linear maps induced by inclusions. Further assuming that $\mathbb{M}$ is compact, we have $\mathbb{M}_{r_0} = \emptyset$ and $\mathbb{M}^{r_0} = \mathbb{M}$, which implies $\mathsf{H}_0 = \mathsf{H}_{2m} = 0$. The sequence of vector spaces is thus

$$0 = \mathsf{H}_0 \to \ldots \to \mathsf{H}_{i-1} \to \mathsf{H}_i \to \ldots \to \mathsf{H}_{j-1} \to \mathsf{H}_j \to \ldots \to \mathsf{H}_{2m} = 0, \tag{10}$$

where $0 < i < j \leq 2m$. Calling this sequence a *tower*, it is *indecomposable* if all vector spaces are trivial except for an interval of 1-dimensional vector spaces, $1 \to \ldots \to 1$, that are connected by isomorphisms. Every tower has a unique decomposition into such intervals. The interpretation is as follows. Assuming the interval starts at position i and ends at position $j-1$, there is a homology class γ *born* at H_i and *dying entering* H_j. We represent this interval by the *birth-death pair* of homological critical values, $A = (\alpha_b, \alpha_d)$, where $\alpha_b = v_i$ or v_{2m-i+1} and $\alpha_d = v_j$ or v_{2m-j+1}, depending on whether $i, j \leq m$ or $m < i, j$. The *dimension* of the birth-death pair is the dimension of the homology group that contains γ, and its *persistence* is $\text{pers}(A) = |\alpha_d - \alpha_b|$. By construction, the rank of H_i is the number of indecomposable towers whose intervals cover position i. The rank of H_i is therefore readily computed from the multiset of birth-death pairs, which we call the *persistence diagram* of f, denoted as $\mathsf{Dgm}(f)$. The number of birth-death pairs with positive persistence is denoted as $\#\mathsf{Dgm}(f)$. It is sometimes useful to take the dimension of the pairs into account. A case in point is a level set of f. To express the ranks of its homology groups in terms of birth-death pairs, we write $\mathsf{Up}_k(f, r_i)$ for the multiset of k-dimensional birth-death pairs with $\alpha_b < r_i < \alpha_d$, and $\mathsf{Dn}_k(f, r_i)$ for the multiset of k-dimensional birth-death pairs with $\alpha_d < r_i < \alpha_b$. With this notation, it can be shown that the rank of the k-th homology group of $f^{-1}(r_i)$ is $\#\mathsf{Up}_k(f, r_i) + \#\mathsf{Dn}_{k+1}(f, r_i)$; see [2]. Since the Euler characteristic is the alternating sum of these ranks, this implies

$$\chi(f^{-1}(r_i)) = \sum_{k=0}^{n} (-1)^k \left(\#\mathsf{Up}_k(f, r_i) - \#\mathsf{Dn}_k(f, r_i) \right). \tag{11}$$

The notions of birth, death, and persistence can also be defined for a tower of vector spaces that may not correspond to a real-valued function on a topological space. This approach is taken in recent papers generalizing the Stability Theorem of persistent homology from functions to towers; see [1, 5]. We assume a 1-parameter family of vector spaces, $\mathcal{F}$, that starts and ends with the trivial vector space, and linear maps from left to right between any two. We call this a *q-tame tower* if all maps have finite rank. Such a tower can be written as the direct sum of indecomposable towers, each characterized by the real values of its birth and its death.

Similar to the notation for functions, we write $\mathsf{Dgm}(\mathcal{F})$ for the persistence diagram of the tower. It is convenient to add infinitely many copies of all trivial birth-death pairs, (α, α) with $\alpha \in \mathbb{R}$, as this simplifies the statement of stability, which we explain next. Let $\mathcal{F}$ and $\mathcal{G}$ be two q-tame towers, writing F_t and G_t for their vector spaces, $t \in \mathbb{R}$. For $\varepsilon > 0$, the two towers are *ε-interleaved* if there are maps $\mathsf{F}_t \to \mathsf{G}_{t+\varepsilon}$ and $\mathsf{G}_t \to \mathsf{F}_{t+\varepsilon}$, for all $t \in \mathbb{R}$, that commute with the maps within the towers. For example, if $\mathcal{F}$ and $\mathcal{G}$ are derived from functions $f, g\colon \mathbb{M} \to \mathbb{R}$, then $\mathcal{F}$ and $\mathcal{G}$ are ε-interleaved for $\varepsilon = \sup_{x\in\mathbb{M}} |f(x) - g(x)|$. We will make essential use of the following assertion of stability. It measures the distance between two birth-death pairs $A = (\alpha_b, \alpha_d)$ and $A' = (\alpha'_b, \alpha'_d)$ as $\|A - A'\|_\infty = \max\{|\alpha_b - \alpha'_b|, |\alpha_d - \alpha'_d|\}$. Note that $|\mathrm{pers}(A) - \mathrm{pers}(A')| \leq 2\|A - A'\|_\infty$.

Theorem 1 (Stability Theorem [1, 5, 7]) *Let $\mathcal{F}$ and $\mathcal{G}$ be q-tame towers, and $\varepsilon > 0$ such that $\mathcal{F}$ and $\mathcal{G}$ are ε-interleaved. There there is a bijection $\beta\colon \mathsf{Dgm}(\mathcal{F}) \to \mathsf{Dgm}(\mathcal{G})$ such that $\|A - \beta(A)\|_\infty \leq \varepsilon$ for all $A \in \mathsf{Dgm}(\mathcal{F})$.*

3 Modified Intrinsic Volume

In this section, we introduce new digital algorithms for the intrinsic volume, defined using Crofton's formula (8). Beginning with the first intrinsic volume, we consider two generalizations, one invariant under rigid motions and the other under rotations about the origin.

Moments. For a height function, $f\colon \mathbb{M} \to \mathbb{R}$, we get a tower of homology groups as explained above. Denoting this tower as $\mathcal{H}$, we get a persistence diagram, $\mathsf{Dgm}(\mathcal{H})$. Restricting our attention to the k-dimensional groups, we get a persistence diagram, $\mathsf{Dgm}_k(\mathcal{H})$, for each dimension k. Motivated by (11), we use the diagrams to introduce an alternating sum of moments. Specifically, the *χ-moment* of *order j* of $\mathcal{H}$ is

$$X^j(\mathcal{H}) = \sum_{k=0}^{n} (-1)^k \sum_{A} \int_{r=\alpha_b}^{\alpha_d} |r|^{j-1} \,\mathrm{d}r, \tag{12}$$

where in the second sum, $A = (\alpha_b, \alpha_d)$ varies over all points in $\mathsf{Dgm}_k(\mathcal{H})$. For $j = 1$, the integral in (12) evaluates to $\alpha_d - \alpha_b$, which for $\alpha_b < \alpha_d$ is the persistence and for $\alpha_d < \alpha_b$ the negative persistence of A. Writing $X(\mathcal{H}) = X^1(\mathcal{H})$, we thus get $X(\mathcal{H}) = \int_{r=-\infty}^{\infty} \chi(f^{-1}(r))\,\mathrm{d}r$; compare (12) with (11). For general order $j \geq 1$, we have $X^j(\mathcal{H}) = \int_{r=-\infty}^{\infty} \chi(f^{-1}(r))|r|^{j-1}\,\mathrm{d}r$. The contribution of A to this integral multiplied with j is

$$j \cdot \int_{r=\alpha_b}^{\alpha_d} |r|^{j-1}\,\mathrm{d}r = \begin{cases} |\alpha_d^j| - |\alpha_b^j| & \text{if } 0 \leq \alpha_b \text{ and } 0 \leq \alpha_d, \\ |\alpha_b^j| - |\alpha_d^j| & \text{if } \alpha_b \leq 0 \text{ and } \alpha_d \leq 0, \\ |\alpha_d^j| + |\alpha_b^j| & \text{if } \alpha_b \leq 0 \leq \alpha_d, \\ -|\alpha_d^j| - |\alpha_b^j| & \text{if } \alpha_d \leq 0 \leq \alpha_b. \end{cases} \tag{13}$$

In addition to these moments, we consider the *modified χ-moment* of *order* j and $\varepsilon > 0$, denoted as $X^j(\mathcal{H}, \varepsilon)$, which is defined as the unmodified χ-moment in (12) except that contributions of birth-death pairs with persistence less than or equal to ε are dropped.

Motion invariant construction. Recall that (9) writes the $(n-k)$-th intrinsic volume as a double integral over all linear k-planes, L, and all k-planes parallel to L. Setting $k = n-1$, the inner integral is over a 1-parameter family of hyperplanes. We introduce the *height function* $f_L \colon \mathbb{M} \to \mathbb{R}$ defined by mapping x to $f_L(x) = \langle x, u \rangle$, in which u denotes the unit normal vector of L. Extending [6], we can therefore rewrite (9) in terms of preimages and χ-moments:

$$V_1(\mathbb{M}) = c_{n-1,n} \cdot \int_{L \in \mathcal{L}^n_{n-1}} \int_{y=-\infty}^{\infty} \chi\left(f_L^{-1}(y)\right) \,\mathrm{d}y \,\mathrm{d}L \tag{14}$$

$$= c_{n-1,n} \cdot \int_{L \in \mathcal{L}^n_{n-1}} X(\mathcal{F}_L) \,\mathrm{d}L, \tag{15}$$

where $\mathcal{F}_L$ is the tower defined by f_L. Finally, we substitute the modified for the unmodified moment to get a modified notion of the first intrinsic volume.

Definition 1 *The modified first intrinsic volume of $\mathbb{M} \subseteq \mathbb{R}^n$ and $\varepsilon > 0$ is*

$$V_1(\mathbb{M}, \varepsilon) = c_{n-1,n} \cdot \int_{L \in \mathcal{L}^n_{n-1}} X(\mathcal{F}_L, \varepsilon) \,\mathrm{d}L. \tag{16}$$

The definition of modified first intrinsic volume is invariant under rigid motions. To generalize this definition to other intrinsic volumes, we note that the integral of $\chi(\mathbb{M} \cap E)$ over all $E \in \mathcal{E}^n_k$ is the same as over all $P \in \mathcal{E}^n_{k+1}$ and then over all $E \in \mathcal{E}^P_k$. Indeed, the measure of $(k+1)$-planes P that contain a given k-plane is $\nu_k(\mathcal{L}^{n-k}_1) = 1$. For each $(k+1)$-plane, P, we fix an origin, consider a k-plane L in P that passes through this origin, let $f_L \colon \mathbb{M} \cap P \to \mathbb{R}$ be the height function in the direction normal to L, and write $\mathcal{F}_L$ for the corresponding tower.

Definition 2 *For $0 \leq k \leq n$, the motion invariant modification of the $(n-k)$-th intrinsic volume of a set $\mathbb{M} \subseteq \mathbb{R}^n$ and $\varepsilon > 0$ is*

$$V^{\mathrm{mot}}_{n-k}(\mathbb{M}, \varepsilon) = c_{k,n} \cdot \int_{P \in \mathcal{E}^n_{k+1}} \int_{L \in \mathcal{L}^P_k} X(\mathcal{F}_L, \varepsilon) \,\mathrm{d}L \,\mathrm{d}P. \tag{17}$$

Note that $V^{\mathrm{mot}}_1(\mathbb{M}, \varepsilon) = V_1(\mathbb{M}, \varepsilon)$ implying that the motion invariant modification is indeed a generalization of the modification of the first intrinsic volume. We have not been able to prove the convergence of $V^{\mathrm{mot}}_{n-k}(\mathbb{M}, \varepsilon)$ for $n-k > 1$, not even for the unit ball, which motivates us to give a different, rotation invariant generalization of (16).

Rotation invariant construction. Let $\varphi\colon \mathcal{E}^n_k \to [0,\infty)$ be a measurable function and $1 \le k < \ell \le n$. Writing $\|E\|$ for the distance between the origin and its closest point on E, we find the following special case of the Blaschke-Petkantschin Formula in [14, Theorem 2.7]:

$$\int_{E\in\mathcal{E}^n_k} \varphi(E)\,\mathrm{d}E = \frac{s_{n-k}}{s_{\ell-k}} \cdot \int_{L\in\mathcal{L}^n_\ell} \int_{E\in\mathcal{E}^L_k} \varphi(E)\,\|E\|^{n-\ell}\,\mathrm{d}E\,\mathrm{d}L, \tag{18}$$

where we recall that s_k is the measure of the $(k-1)$-dimensional sphere. Grouping the k-planes in 1-parameter families, we are interested in the case $\ell = k+1$, for which we get $s_{\ell-k} = s_1 = 2$ in the denominator. Setting $\varphi(E) = \chi(\mathbb{M}\cap E)$, we first use (18) and then (9) to rewrite (8) as

$$V_{n-k}(\mathbb{M}) = \tfrac{1}{2}c_{k,n}s_{n-k} \cdot \int_{L\in\mathcal{L}^n_{k+1}} \int_{E\in\mathcal{E}^L_k} \chi(\mathbb{M}\cap E)\,\|E\|^{n-k-1}\,\mathrm{d}E\,\mathrm{d}L \tag{19}$$

$$= \tfrac{1}{2}c_{k,n}s_{n-k} \cdot \int_{L\in\mathcal{L}^n_{k+1}} \int_{K\in\mathcal{L}^L_k} \int_{y\in K^\perp} \chi\left(\mathbb{M}\cap(K+y)\right)\,|y|^{n-k-1}\,\mathrm{d}y\,\mathrm{d}K\,\mathrm{d}L \tag{20}$$

$$= \tfrac{1}{2}c_{k,n}s_{n-k} \cdot \int_{L\in\mathcal{L}^n_{k+1}} \int_{K\in\mathcal{L}^L_k} \int_{y=-\infty}^{\infty} \chi\left(f_K^{-1}(y)\right)\,|y|^{n-k-1}\,\mathrm{d}y\,\mathrm{d}K\,\mathrm{d}L \tag{21}$$

$$= \tfrac{1}{2}c_{k,n}s_{n-k} \cdot \int_{L\in\mathcal{L}^n_{k+1}} \int_{K\in\mathcal{L}^L_k} X^{n-k}(\mathcal{F}_K)\,\mathrm{d}K\,\mathrm{d}L. \tag{22}$$

We get (21) by introducing the function $f_K\colon \mathbb{M}\cap L \to \mathbb{R}$ that maps x to the height $f_K(x)$ in the normal direction u of K inside L. Observe that $f_K^{-1}(y)$ is the intersection of $\mathbb{M}$ with the k-plane $K+y$ parallel to K. Finally, we get (22) using the χ-moment of order $n-k$ of f_K. We modify the intrinsic volume by substituting the modified for the unmodified χ-moment.

Definition 3 *For $0 \le k \le n-1$, the rotation invariant modification of the $(n-k)$-th* intrinsic volume *of $\mathbb{M}\subseteq\mathbb{R}^n$ and $\varepsilon > 0$ is*

$$V^{\mathrm{rot}}_{n-k}(\mathbb{M},\varepsilon) = \tfrac{1}{2}c_{k,n}s_{n-k} \cdot \int_{L\in\mathcal{L}^n_{k+1}} \int_{K\in\mathcal{L}^L_k} X^{n-k}(\mathcal{F}_K,\varepsilon)\,\mathrm{d}K\,\mathrm{d}L. \tag{23}$$

Equation (23) accumulates information by probing $\mathbb{M}$ with all $(k+1)$-planes that pass through the origin, which implies that the construction is invariant under rotations about the origin. Note that $V^{\mathrm{rot}}_1(\mathbb{M},\varepsilon) = V_1(\mathbb{M},\varepsilon)$ implying that the rotation invariant modification is indeed a generalization of the modified first intrinsic volume.

4 Convergence for Balls

In this section, we show that the rotation invariant modification of the intrinsic volumes implies multigrid convergent digital algorithms for the n-dimensional ball,

thus correcting the non-convergence we observed in our motivating example. The proof of convergence first constructs a map from $\mathbb{B}^n$ to $\mathbb{B}^n_t$, and second bounds the difference between the modified and unmodified intrinsic volumes using the Stability Theorem of persistent homology.

Low-distortion mapping. Recall that $\mathbb{B}^n \cap t\mathbb{Z}^n$ is the resolution t digitization of the unit ball, and $\mathbb{B}^n_t$ is the union of axes-aligned n-cubes with edge length t and centers in $\mathbb{B}^n \cap t\mathbb{Z}^n$. The intersection of this union of cubes with a line may have more than one component, but this cannot be the case if the line passes through the origin. We use this fact to construct a low-distortion homeomorphism between $\mathbb{B}^n$ and $\mathbb{B}^n_t$. Denoting the homeomorphism by $h_t \colon \mathbb{B}^n \to \mathbb{B}^n_t$, we define its *distortion* as $\sup_{x\in\mathbb{B}^n} \|x - h_t(x)\|$.

Lemma 1 (Mapping Lemma) *For every positive real t, there is a homeomorphism $h_t \colon \mathbb{B}^n \to \mathbb{B}^n_t$ with distortion at most $\frac{1}{2}t\sqrt{n}$ such that for every linear subspace L of $\mathbb{R}^n$, the restriction of h_t to $\mathbb{B}^n \cap L \to \mathbb{B}^n_t \cap L$ is again a homeomorphism.*

Proof. We begin by showing that every line $K \in \mathcal{L}^n_1$ intersects $\mathbb{B}^n_t$ in a single component. Indeed, if this were not the case, then we could find two neighboring n-cubes, U and U' with centers u and u', such that $U \notin \mathbb{B}^n_t$, $U' \subseteq \mathbb{B}^n_t$, and $\|u\| < \|u'\|$. This contradicts the definition of hit-or-miss digitization and implies that $\mathbb{B}^n_t$ is star-convex with the origin in the kernel. We exploit this property in the construction of the homeomorphism $h_t \colon \mathbb{B}^n \to \mathbb{B}^n_t$. Using the coordinate system along K, we write the intersections with the two bodies as intervals: $K \cap \mathbb{B}^n = [-1, 1]$ and $K \cap \mathbb{B}^n_t = [-a, a]$. To map the former interval to the latter, we set $h_t(y) = ay$ for every $y \in [-1, 1]$. Doing this for all lines passing through the origin defines the homeomorphism. To quantify its distortion, we note that the distance between a and 1 is at most half the length of a cube diagonal, which implies that the distortion of h_t is at most $\frac{1}{2}t\sqrt{n}$. The star-convexity of the digital approximation implies that $\mathbb{B}^n_t \cap L$ is a topological ball of dimension k for every $L \in \mathcal{L}^n_k$. By construction of the homeomorphism, the corresponding restriction of h_t is a homeomorphism, as required. ◻

Integration. Fixing a direction, we let $f \colon \mathbb{B}^n \to \mathbb{R}$ be the height function on the unit ball, and we let $g \colon \mathbb{B}^n \to \mathbb{R}$ be defined by mapping $x \in \mathbb{B}^n$ to the height of $h_t(x) \in \mathbb{B}^n_t$ in the same direction. We write $\mathcal{F}$ and $\mathcal{G}$ for the corresponding towers of homology groups, and $\mathsf{Dgm}(\mathcal{F})$ and $\mathsf{Dgm}(\mathcal{G})$ for their persistence diagrams. Setting $c = \frac{1}{2}t\sqrt{n}$, we have $\sup_{x\in\mathbb{B}^n} |f(x) - g(x)| \leq c$ by the Mapping Lemma. It follows that there is a bijection between the two multisets of birth-death pairs with distance at most c between corresponding pairs. Note that $\mathsf{Dgm}(\mathcal{F})$ has only one non-trivial pair, namely $A = (-1, 1)$. By the Stability Theorem, A corresponds to a pair $A' = (-a, a)$ with $1 - c \leq a \leq 1 + c$ in $\mathsf{Dgm}(\mathcal{G})$. All other pairs in $\mathsf{Dgm}(\mathcal{G})$ correspond to trivial pairs in $\mathsf{Dgm}(\mathcal{F})$. Except for A', all pairs in $\mathsf{Dgm}(\mathcal{G})$

have persistence $2c$ or less. Setting $\varepsilon = 2c$, there is only one contribution to the modified χ-moment, $X^{n-k}(\mathcal{G}, \varepsilon)$, namely that of A', which is

$$\int_{r=-a}^{a} |r|^{n-k-1} \, \mathrm{d}r = \frac{2a^{n-k}}{n-k} < \frac{2e^{c(n-k)}}{n-k}. \tag{24}$$

Comparing this to the unmodified χ-moment of $\mathcal{F}$, which is $X^{n-k}(\mathcal{F}) = \frac{2}{n-k}$, we see that the difference is less than $(2e^{c(n-k)} - 2)/(n-k)$. To compute the difference between the intrinsic volumes, we still need to integrate over all $L \in \mathcal{L}^n_{k+1}$ and $K \in \mathcal{L}^L_k$ and multiply with $\frac{1}{2} c_{k,n} s_{n-k}$; see (23).

Theorem 2 (Convergence Theorem for Balls) *The absolute difference between the $(n-k)$-th intrinsic volume of $\mathbb{B}^n$ and the rotation invariant modification of the $(n-k)$-th intrinsic volume of its resolution t digital approximation is*

$$|V_{n-k}(\mathbb{B}^n) - V^{\mathrm{rot}}_{n-k}(\mathbb{B}^n_t, t\sqrt{n})| \leq \tfrac{1}{n-k} c_{k,n} s_{n-k} \cdot \left(e^{\frac{t\sqrt{n}(n-k)}{2}} - 1 \right) \tag{25}$$

for $0 \leq k < n$. The difference vanishes as t goes to 0, hence $\lim_{t \to 0} V^{\mathrm{rot}}_{n-k}(\mathbb{B}^n_t, t\sqrt{n}) = V_{n-k}(\mathbb{B}^n)$.

This theorem implies a digital algorithm that is multigrid convergent for $\mathcal{S} = \{\mathbb{B}^n\}$. It is easy to extend the proof to show that the same algorithm is multigrid convergent for all ellipsoids centered at the origin. It may even be multigrid convergent for all convex sets that contain the origin in their interiors, but we do not have a proof.

5 Distorted Normals of the Sphere

In this section, we introduce the main technical tool used to prove our second convergence result in Section 7. The distorted normal bundle of a body is a modification of the usual normal bundle and is of independent interest. We begin by introducing the notion for the special case of a sphere.

Distorted normal map. To explain the construction, we recall that the outward normal of a point $u \in \mathbb{S}^{n-1}$ may be written as $N(u) = u - 0$, in which 0 is the center of the sphere. We distort by substituting the n-dimensional cube $\square^n = [-1, 1]^n / \sqrt{4n}$ for 0. The edges of $\square^n$ have length $1/\sqrt{n}$, and its corners are at distance $\frac{1}{2}$ from 0 and from $\mathbb{S}^{n-1}$. For each point $u \in \mathbb{S}^{n-1}$, let $u_\square \in \square^n$ be the closest point in the n-cube. Writing u_i for the i-th Cartesian coordinate of u, we call it *small* if $|u_i| \leq 1/\sqrt{4n}$ and *large* if $|u_i| > 1/\sqrt{4n}$. The i-th coordinate of $u_\square$ is given by

$$u_{\square i} = \begin{cases} u_i & \text{if } u_i \text{ is small,} \\ \pm 1/\sqrt{4n} & \text{if } u_i \text{ is large.} \end{cases} \tag{26}$$

We observe that $u - u_\square$ is an *outward normal* of $\partial \square^n$, meaning the orthogonal $(n-1)$-plane that passes through $u_\square$ separates the n-cube from the difference vector.

Definition 4 *The distorted normal map,* $D_n\colon \mathbb{S}^{n-1} \to \mathbb{S}^{n-1}$*, is defined by mapping every point* $u \in \mathbb{S}^{n-1}$ *to* $D_n(u) = (u - u_\square)/\|u - u_\square\|$.

To visualize D_n, we first consider the *minimum distance function*, $d_n\colon \mathbb{S}^{n-1} \to \mathbb{R}$, defined by mapping $u \in \mathbb{S}^{n-1}$ to $d_n(u) = \|u - u_\square\|$. It decomposes the sphere into regions of points whose closest points belong to the same face of the n-cube. As illustrated in Figure 1, we have $3^n - 1$ regions, one for each proper face of $\square^n$. These

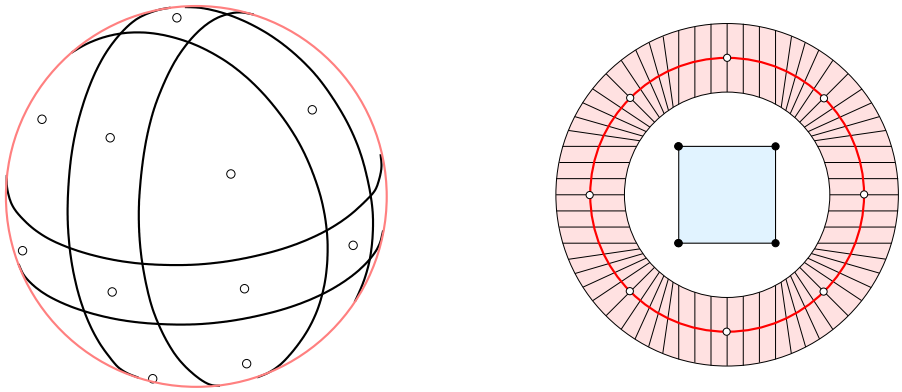

Figure 1: *Left:* the decomposition of $\mathbb{S}^2$ into regions. *Right:* the decomposition of $\mathbb{S}^1$ together with the annulus, which is the union of the distorted normal segments. The center of each region is a critical point of the minimum distance function and a fixed point of the distorted normal map.

regions arise by intersecting $\mathbb{S}^{n-1}$ with the $2n$ $(n-1)$-planes that contain the $(n-1)$-faces of $\square^n$. Within each region, the distance function has a simple form, with a critical point at its center. For an $(n-1)$-face, this critical point is a maximum, for a vertex it is a minimum, and for every other proper face it is a saddle point whose index depends on the dimension of the face. Each critical point of d_n is a fixed point of D_n, and these are the only fixed points.

The angles cannot be large. The following two angles are useful in the analysis of of the distorted normal map: $\varphi_n = \arcsin \sqrt{1/(4n)}$ and $\psi_n = \arccos \sqrt{(3n+1)/(4n)}$. The first angle gives the maximum deviation from orthogonality below which the distortion enforces precise orthogonality to a coordinate direction; it decreases with increasing n and vanishes in the limit. The second angle gives the maximum distortion; it increases with increasing n and goes to $30°$ in the limit. We formally state and prove both properties together with a bound on the angle between distorted normals. Write e_1 to e_n for the unit coordinate vectors in $\mathbb{R}^n$.

Lemma 2 *Let* $D_n\colon \mathbb{S}^{n-1} \to \mathbb{S}^{n-1}$ *be the distorted normal map. Then*

(i) $\arcsin |\langle u, e_i\rangle| \le \varphi_n$ *iff* $\langle D_n(u), e_i\rangle = 0$*, for every* $u \in \mathbb{S}^{n-1}$ *and every* $1 \le i \le n$*,*

(ii) $\arccos \langle u, D_n(u)\rangle \le \psi_n$*, for every* $u \in \mathbb{S}^{n-1}$*, and this bound is tight,*

(iii) $\arccos\langle D_n(u), D_n(v)\rangle \leq 2\arccos\langle u, v\rangle$*, for all* $u, v \in \mathbb{S}^{n-1}$.

Proof. (i) says that almost right angles with coordinate directions become right angles. To see this, note that $|\langle u, e_i\rangle| \leq \sin\varphi_n$ iff $u_\square$ belongs to a face parallel to e_i. These faces are characterized by having outward normals orthogonal to e_i.

(ii) implies that the distortion of the normal direction is never more than 30°. To prove the inequality, we consider a region in the decomposition of $\mathbb{S}^{n-1}$, noting that the distortion increases monotonically along great-circle arcs emanating from the fixed point. It follows that the maximum is attained at the corners of the regions, which are the points $v = (v_1, v_2, \ldots, v_n) \in \mathbb{S}^{n-1}$ with $v_j = \pm\cos\psi_n$, for one index j, and $v_i = \pm\sin\varphi_n$, for all indices $i \neq j$. Correspondingly, the j-th coordinate of $D_n(v)$ is ± 1, with the same sign as v_j, and the other coordinates are 0. It follows that $\langle v, D_n(v)\rangle = \cos\psi_n$ at the $n2^n$ corners, and $\langle u, D_n(u)\rangle \leq \cos\psi_n$ at all $u \in \mathbb{S}^{n-1}$.

(iii) says that the angle between two distorted normals is at most twice the angle between the corresponding undistorted normals. To prove this, we consider the derivative of D_n, at every point and every tangent direction at that point. It is maximized at the diagonal point, $u_0 = (\sqrt{1/n}, \sqrt{1/n}, \ldots, \sqrt{1/n})$, whose closest point on the n-cube is $\frac{1}{2}u_0$. To see this, we note that u_0 minimizes the minimum distance function, and the closest point on $\square^n$ is constant within a small neighborhood of u_0. Independent of the tangent direction, the derivative at u_0 is 2, which is a global maximum. To show that the claimed inequality follows, we note that $\arccos\langle u, v\rangle$ is the length of the shortest great-circle arc connecting the two points on $\mathbb{S}^{n-1}$. We map this arc to a curve connecting $D_n(u)$ to $D_n(v)$, observing that its length is at least $\arccos\langle D_n(u), D_n(v)\rangle$. Since the derivative is bounded from above by 2, the length of this curve is at most twice the length of the great-circle arc. ◻

The segments cannot be long. Two line segments that intersect $\mathbb{S}^{n-1}$ orthogonally at different points can only intersect at the origin and are disjoint otherwise. If we draw the line segments in distorted normal direction, then they are disjoint unless they intersect inside $\square^n$. We therefore define $\mathbb{A}(\mathbb{S}^{n-1}) = \mathbb{S}^{n-1} + \frac{1}{4}\mathbb{B}^n$ and draw the line segments in distorted normal direction within this annulus; see Figure 1. More formally, we write $L_u(\lambda) = u + \lambda D_n(u)$ and we define the *distorted normal segment* of $u \in \mathbb{S}^{n-1}$ as

$$L_u = \mathbb{A}(\mathbb{S}^{n-1}) \cap \left\{ L_u(\lambda) \mid -\tfrac{1}{2} < \lambda < \tfrac{1}{2} \right\}. \tag{27}$$

We prove shortly that each L_u is a connected line segment whose endpoints lie on the boundary of the annulus.

Lemma 3 $\mathbb{A}(\mathbb{S}^{n-1})$ *is a disjoint union of distorted normal segments.*

Proof. By construction, $\mathbb{A}(\mathbb{S}^{n-1})$ and $\square^n$ are disjoint, which implies that the distorted normal segments are pairwise disjoint. It remains to prove that the distorted normals cover the annulus. This requires two things: the distorted normals should

be dense enough to cover the interior of the annulus, and they should be long enough to reach the boundary. The first property holds because the midpoints of the distorted normals cover $\mathbb{S}^{n-1}$. In the remainder of the proof we establish the second property.

To prove that L_u is connected and its endpoints lie on the boundary of the annulus, we compute the distance of $L_u(\lambda)$ from $\mathbb{S}^{n-1}$, which depends on λ and the angle $\alpha = \arccos\langle N(u), D_n(u)\rangle$ between the normal and the distorted normal. It is convenient to measure the distance with a sign, which is negative inside and positive outside $\mathbb{S}^{n-1}$. Writing $d_u\colon \mathbb{R} \to \mathbb{R}$ for the signed distance function along the distorted normal segment of u, we see from the right-angled triangle in Figure

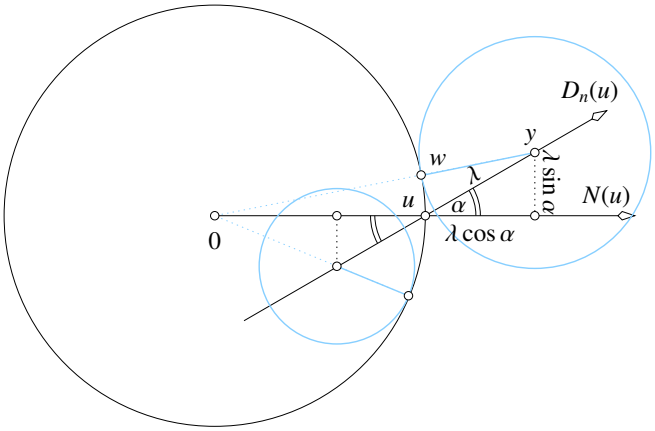

Figure 2: Illustration of the proof of Lemma 3. Point y is at a positive distance λ from u in the distorted normal direction. Noting that $d_u(\lambda) = \|w - y\|$, the distance to the sphere is computed from the right-angled triangle with shown edge lengths. Similar computations apply for negative values of λ.

2 that $d_u(\lambda) = \sqrt{1 + 2\lambda\cos\alpha + \lambda^2} - 1$. It attains its minimum at $\lambda = -\cos\alpha$, has a root at $\lambda = 0$, and increases monotonically for $\lambda \geq -\cos\alpha$. Varying α, we note that we get smaller absolute distances for larger angles. Since $\alpha \leq \frac{\pi}{6}$, this implies

$$|d_u(\lambda)| \geq \sqrt{1 + \sqrt{3}\lambda + \lambda^2} - 1. \tag{28}$$

For $\lambda = \pm 0.5$, we get $d_u(-0.5) \leq -0.380\ldots$ and $d_u(0.5) \geq 0.454\ldots$. Both have absolute value larger than 0.25, which implies that the points $L_u(\lambda)$ on the boundary of $\mathbb{A}(\mathbb{S}^{n-1})$ satisfy $-\frac{1}{2} < \lambda < \frac{1}{2}$, and the distorted normal segment L_u, as defined in (27), crosses the annulus from one boundary sphere to the other, as required. ◻

The vectors cannot disagree. By construction, the endpoints of the distorted normal segments lie on two spheres centered at the origin, and by Lemma 3, these segments establish homeomorphic maps between $\mathbb{S}^{n-1}$ and the two spheres. We are interested in the differential properties of these maps. To study them, we consider

a smooth curve of directions, $\upsilon\colon \mathbb{R} \to \mathbb{S}^{n-1}$, set $u = \upsilon(0)$, and write $\vec{u} = \dot{\upsilon}(0)$ for the velocity vector at u. As a first step toward understanding the curves traced out by the endpoints of the distorted normal segments, we consider $S = \frac{3}{4}\mathbb{S}^{n-1}$, and let $\phi\colon \mathbb{R} \to S$ be the curve defined by mapping t to $\phi(t) = (1 - \lambda(t))\upsilon(t) + \lambda(t)u_\square$, in which $0 \le \lambda(t) \le 1$ is chosen so that the point lies on S. Assuming differentiability at 0, we write $\vec{p} = \dot{\phi}(0)$ for the velocity vector at $p = \phi(0)$. To simplify the statement of the claim, we set $\eta_1 = \arccos\frac{1}{2} - \arccos\frac{2}{3} = 11.810\ldots^\circ$.

Lemma 4 *Let $\upsilon\colon \mathbb{R} \to \mathbb{S}^{n-1}$, $\phi\colon \mathbb{R} \to S$ be the curves introduced above, set $u = \upsilon(0)$, $p = \phi(0)$, and let $\vec{u} = \dot{\upsilon}(0)$, $\vec{p} = \dot{\phi}(0)$ be the velocity vectors. Then* $\arccos\langle \vec{u}/\|\vec{u}\|, \vec{p}/\|\vec{p}\|\rangle \le \eta_1$.

Proof. We prove the inequality by relating the angle between the velocity vectors to the angle between the normals of the $(n-1)$-planes, H, G, that touch $\mathbb{S}^{n-1}$ in u and S in p. Consider the triangle with vertices $p, 0, u$ and write $\alpha = \angle p0u$ for the angle at the origin. By construction, $\|0 - u\| = 1$ and $\|0 - p\| = \frac{3}{4}$, and by Lemma 2 (ii), the angle at u satisfies $\angle pu0 \le \frac{\pi}{6}$. To prove an upper bound on α, we may assume $\angle pu0 = \frac{\pi}{6}$, which specifies the triangle up to congruence. It is now easy to check that in this extreme configuration the angle at 0 is $\eta_1 = \arccos\frac{1}{2} - \arccos\frac{2}{3}$.

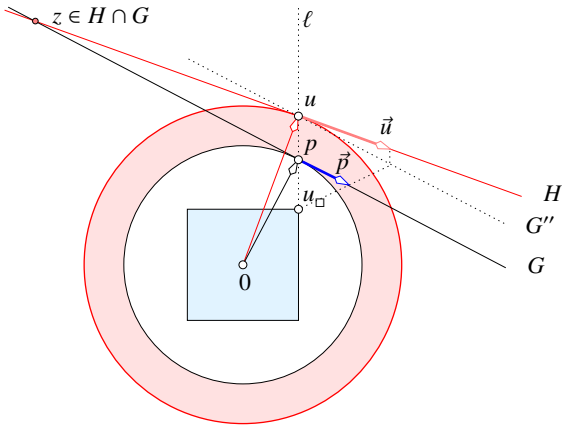

Figure 3: Illustration of the proof of Lemma 4. The points u, p and the velocity vectors $\vec{u}, \vec{p}$ are related to each other by parallel projection from H to G'' followed by central projection from G'' to G. The vectors u, p are normal to H, G.

Having established an upper bound on the angle between the normals of H and G, we return to the velocity vectors at u and p. To get $p + \vec{p}$ from $u + \vec{u}$, we define $G'' = G + (u - p)$, we project $u + \vec{u}$ parallel to $p - u$ from H to G'', and we finally project the point in G'' in the direction toward $u_\square$ onto G; see Figure 3. To analyze the situation, let ℓ be the line that passes through u, p, and we remember that H, G touch two concentric spheres. It follows that the 2-plane passing through $u, p, 0$ intersects the $(n-2)$-plane $H \cap G$ orthogonally at a point z. Any other 2-plane containing u, p intersects $H \cap G$ at a point z' whose distance from ℓ is larger than the distance of z from ℓ. Assuming $u, u + \vec{u}$ and $p, p + \vec{p}$ lie in the 2-plane

defined by z', the angle between $\vec{u}, \vec{p}$ is the same as the angle between $u - z'$ and $p - z'$. This angle is maximized when the distance to the line is minimized, which happens when $z' = z$. To see this, we consider the circle that passes through u, p, z. Moving z on its arc bounded by u and p, or moving it with the circle as it pivots about the line ℓ does not change the angle. (This is known as the Inscribed Angle Theorem.) Drawing all circles of the same size that pass through u, p, we get a self-intersecting torus that passes through z. A portion of the torus lies on the boundary of its convex hull. We get this portion by cutting each circle with the line parallel to ℓ that passes through its center, removing the half that contains u and p, and taking the union of the remaining half-circles. Importantly, z belongs to this portion of the torus because the angles at u and p within the triangle spanned by u, p, z are both at least $\frac{\pi}{3} - \eta_1$, which is larger than 45°. The $(n-2)$-plane $H \cap G$ touches this portion of the torus in a single point, which is z. Outside the torus, the angles are smaller, which implies that the angle is indeed maximized at z, where it is equal to the angle between the normals of the two $(n-1)$-planes, which is at most η_1, as claimed. ◻

The vectors cannot swing. As a second step toward understanding the curves traced out by the endpoints of the distorted normal segments, we let $\psi\colon \mathbb{R} \to S$ be defined by $\psi(t) = \upsilon(t) + \mu(t) D_n(\upsilon(t))$, in which $-1 \le \mu(t) \le 0$ is chosen so that the point lies on S. We have differentiability at 0 if u lies in the interior of a region on $\mathbb{S}^{n-1}$ that projects to a face of $\square^n$; see Figure 1. Assuming differentiability, we let $\vec{q} = \dot{\psi}(0)$ be the velocity vector at $q = \psi(0)$. If all coordinates of u are large, then $\psi(t) = \phi(t)$ in a neighborhood of 0, and therefore $\vec{p} = \vec{q}$. Otherwise, the two velocity vectors are different. To simplify the statement of the claim, we set $\eta_2 = \arccos(2\sqrt{2})/3 = 19.471\ldots°$.

Lemma 5 *Let $\phi\colon \mathbb{R} \to S$, $\psi\colon \mathbb{R} \to S$ be the curves obtained from $\upsilon\colon \mathbb{R} \to \mathbb{S}^{n-1}$ as described above, set $p = \phi(0)$, $q = \psi(0)$, assume differentiability at 0, and let $\vec{p} = \dot{\phi}(0)$, $\vec{q} = \dot{\psi}(0)$ be the velocity vectors. Then* $\arccos \langle \vec{p}/\|\vec{p}\|, \vec{q}/\|\vec{q}\| \rangle \le \eta_2$.

Proof. Assume without loss of generality that the first k coordinates of u are small, and the last $n - k$ are large. Writing u_i, p_i, q_i for the i-th coordinates of $\vec{u}, \vec{p}, \vec{q}$, we therefore have

$$q_i = \begin{cases} u_i & \text{if } 1 \le i \le k, \\ p_i & \text{if } k < i \le n. \end{cases} \tag{29}$$

Consider the former case and note that the first k coordinates of the vector $u - u_\square$ are zero. It follows that $p_i = u_i/E$, with $E = \|u - u_\square\|/\|p - u_\square\|$, for $1 \le i \le k$. Equivalently, $q_i = E p_i$ for $1 \le i \le k$. The ratio of distances is largest when u lies on the diagonal, in which case $\|u - u_\square\| = 2\|p - u_\square\|$. Hence, $E \le 2$ in general. To

compute the angle between $\vec{p}$ and $\vec{q}$, we assume $\|\vec{p}\| = 1$ and get

$$\arccos \langle \vec{p}, \frac{\vec{q}}{\|\vec{q}\|} \rangle = \arccos \frac{E \sum_{i=1}^{k} p_i^2 + \sum_{i=k+1}^{n} p_i^2}{\sqrt{E^2 \sum_{i=1}^{k} p_i^2 + \sum_{i=k+1}^{n} p_i^2}} \tag{30}$$

$$= \arccos \frac{1 + (E-1) \sum_{i=1}^{k} p_i^2}{\sqrt{1 + (E^2-1) \sum_{i=1}^{k} p_i^2}} \tag{31}$$

$$\leq \arccos \frac{1 + (E-1)/(E+1)}{\sqrt{1 + (E^2-1)/(E+1)}}, \tag{32}$$

in which get the last line by observing that for fixed E the angle attains its maximum when $\sum_{i=1}^{k} p_i^2 = \frac{1}{E+1}$. The expression simplifies to $\arccos(2\sqrt{E})/(E+1)$, which increases with increasing E. Recall that $E \leq 2$, which implies that the angle is bounded from above by $\arccos(2\sqrt{2})/3 = \eta_2$, as claimed. □

Putting the inequalities of Lemmas 4 and 5 together, we conclude that the angle between $\vec{u}$ and $\vec{q}$ is bounded from above by $\eta_1 + \eta_2 = 31.281\ldots^\circ$.

6 Distorted Normals of a Solid Body

In this section, we extend distorted normals from the sphere to more general sets. We introduce the notion of a solid body and study how it relates to its digital approximations.

Solid bodies. We call a compact set $\mathbb{M} \subseteq \mathbb{R}^n$ an *n-dimensional solid body* if

I. its boundary is a smoothly embedded $(n-1)$-dimensional manifold in $\mathbb{R}^n$, and

II. every height function on $\mathbb{M}$ has a finite size persistence diagram.

We use quantified versions of Properties I and II to constrain the sets we work with. To explain this, let $f_u : \mathbb{M} \to \mathbb{R}$ be the height function on $\mathbb{M} \subseteq \mathbb{R}^n$ in direction u, and recall that $\#\mathsf{Dgm}(f_u)$ denotes the number of birth-death pairs with positive persistence. We require that there exists a constant C such that $\#\mathsf{Dgm}(f_u) \leq C$ for every direction $u \in \mathbb{S}^{n-1}$. Since $\partial\mathbb{M}$ is a smoothly embedded manifold, sectional curvatures are defined, and we write $\mathrm{curv}(\partial\mathbb{M})$ for the maximum sectional curvature, over all points $x \in \partial\mathbb{M}$ and all tangent directions of $\partial\mathbb{M}$ at x. This notion of curvature is related to the *reach* of $\partial\mathbb{M}$, which is the supremum over all r such that every point at distance at most r has a unique closest point on $\partial\mathbb{M}$. Specifically, we have $\mathrm{reach}(\partial\mathbb{M}) \leq 1/\mathrm{curv}(\partial\mathbb{M})$. We do not necessarily have equality because the reach may be determined by a global feature of the embedding in which two points that are far apart in $\partial\mathbb{M}$ are close in $\mathbb{R}^n$. If $\partial\mathbb{M}$ is compact and smoothly embedded, then $\mathrm{curv}(\partial\mathbb{M})$ and $\mathrm{reach}(\partial\mathbb{M})$ are both positive. We require that $1/\mathrm{curv}(\partial\mathbb{M}) \geq 4tn$

and reach($\partial\mathbb{M}$) $\geq 2t\sqrt{n}$, in which t is the resolution of the digital approximation. In other words, we make statements only about approximations for which the resolution is small enough to satisfy these requirements. As a short-cut we sometimes write ϱ for reach($\partial\mathbb{M}$).

A crucial concept in the proof of convergence will be the *annulus* obtained by thickening the boundary of $\mathbb{M}$: $\mathbb{A}_\theta(\partial\mathbb{M}) = \partial\mathbb{M} + \theta\mathbb{B}^n$. For $\theta <$ reach($\partial\mathbb{M}$), we can construct the annulus as the disjoint union of normal segments of the form $x+\lambda N(x)$ for $-\theta \leq \lambda \leq \theta$. The segments establish a bijection between the inner and outer boundaries of the annulus, which we denote as $\partial_{\mathrm{i}}\mathbb{A}_\theta$ and $\partial_{\mathrm{o}}\mathbb{A}_\theta$. Furthermore, the segments form bijections between $\partial\mathbb{M}$ and the two boundaries, and because $\partial\mathbb{M}$ is smoothly embedded so are $\partial_{\mathrm{i}}\mathbb{A}_\theta$ and $\partial_{\mathrm{o}}\mathbb{A}_\theta$. For sufficiently small θ, we will give a third construction of the annulus as a disjoint union of distorted normal segments. The main purpose of this section is the study of this construction for the special case in which $\theta = \frac{1}{4}$reach($\partial\mathbb{M}$).

Symmetric difference. The main difficulty in proving convergence of the modified first intrinsic volume is the establishment of a low-distortion correspondence between $\mathbb{M}$ and $\mathbb{M}_t$. To construct it, we focus on the space near the boundaries. Specifically, we consider the symmetric difference, $(\mathbb{M} \setminus \mathbb{M}_t) \cup (\mathbb{M}_t \setminus \mathbb{M})$, which is partially open and partially closed; see Figure 4. Importantly, the distance of

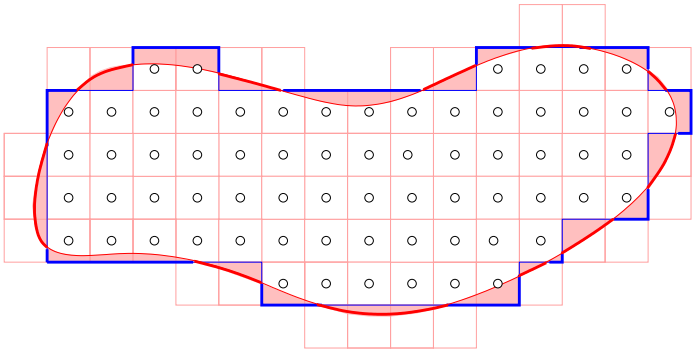

Figure 4: The shaded symmetric difference between $\mathbb{M}$ and $\mathbb{M}_t$, which is contained in the corridor of the cubes that intersect $\partial\mathbb{M}$.

a point of the symmetric difference from $\partial\mathbb{M}$ is at most half the length of a cube diagonal, which is $\frac{1}{2}t\sqrt{n}$. To form the correspondence, we partition the symmetric difference into half-open line segments that have one endpoint on $\partial\mathbb{M}$ and the other endpoint on $\partial\mathbb{M}_t$. However, it is in general not possible to choose the line segments such that they imply a homeomorphism between $\partial\mathbb{M}$ and $\partial\mathbb{M}_t$. To see this, consider a surface $\partial\mathbb{M}$ in $\mathbb{R}^3$ that is locally close to a plane of integer points. More precisely, all but two integer points of this plane lie above $\partial\mathbb{M}$, and the two exceptional points have coordinates (i, j, k) and $(i+1, j+1, k)$. The cubes centered at these two points share a single edge. This edge and the four incident squares belong to $\partial\mathbb{M}_t$, which is therefore not a 2-manifold. Since $\partial\mathbb{M}$ is a 2-manifold by assumption, the two

boundaries cannot be homeomorphic. Giving up on fibrations that imply homeomorphisms, we construct one that implies a homotopy equivalence. The usual normal bundle will not do because there may be points $x \in \partial\mathbb{M}$ with unit outward normal $N(x)$ such that $x + \lambda N(x)$ crosses $\partial\mathbb{M}_t$ more than twice in close vicinity to x. Crucially, such normal directions are necessarily almost orthogonal to at least one coordinate direction. This insight was the motivation to construct the distorted normal bundle introduced in the previous section. We adopt this notion for solid bodies, proving that distorted normal segments are disjoint, and they intersect the symmetric difference in connected pieces.

The segments cannot backtrack. To extend distorted normal segments from $\mathbb{S}^{n-1}$ to the boundary of a solid body, $\partial\mathbb{M}$, we let $L_x(\lambda) = x + \lambda D_n(N(x))$ be a point along the distorted normal vector anchored at x. Writing $d_x(\lambda)$ for the signed distance from $L_x(\lambda)$ to $\partial\mathbb{M}$ – as we did for the sphere – we get a function from $\mathbb{R}$ to $\mathbb{R}$. However, we will limit ourselves to $0 \leq \lambda \leq \frac{\varrho}{2}$, and to avoid overloading the notation, we write $d_x \colon [0, \frac{\varrho}{2}] \to \mathbb{R}$.

Lemma 6 *The function d_x increases monotonically, and, for all $0 \leq \lambda \leq \frac{\varrho}{2}$,*

$$\varrho - \sqrt{\varrho^2 - \sqrt{3}\varrho\lambda + \lambda^2} \leq d_x(\lambda) \leq \lambda.$$

Proof. We first prove the two inequalities. Fix a value of λ and write $y = L_x(\lambda)$. The point of $\partial\mathbb{M}$ closest to y lies on or outside the sphere with radius ϱ centered at $z = x + \varrho N(x)$. Hence, $d_x(\lambda)$ is bounded from below by $\varrho - \|y - z\|$ and from above by $\|y - x\| = \lambda$, which gives the claimed upper bound; see Figure 5. Letting α be the angle between $N(x)$ and $D_n(N(x))$, the squared distance between y and z is $\|y - z\|^2 = \varrho^2 - 2\varrho\lambda\cos\alpha + \lambda^2$. Since $\alpha \leq \frac{\pi}{6}$, this implies $\|y - z\|^2 \leq \varrho^2 - \sqrt{3}\varrho\lambda + \lambda^2$ and the claimed lower bound.

To prove monotonicity, we consider the sphere S with center $y = L_x(\lambda)$ and radius $r = d_x(\lambda)$. Let $w \in S$ be a point that permits a sphere of radius ϱ that passes through x, encloses S, and touches S in w. The set of such points is the intersection of S with an $(n-1)$-plane, H, orthogonal to the distorted normal vector, and we set $\lambda_0 \in \mathbb{R}$ such that $\langle w, D_n(N(x))\rangle = \lambda_0$. We claim that $\lambda_0 < \lambda$, for all $\lambda \leq \frac{\varrho}{2}$. To see this, we observe that for fixed λ, λ_0 is maximized if the radius r of S is as small as possible. We can therefore restrict ourselves to the case in which S touches the sphere centered at z. But then the point at which the two spheres meet satisfies the requirements for w and therefore belongs to H. Letting $\alpha = \angle yxz$ and $\beta = \angle xzy$ bet the angles at x and z, we have $\lambda_0 < \lambda$ as long as $\alpha + \beta < \frac{\pi}{2}$. We have $\alpha \leq \frac{\pi}{6}$ by Lemma 2 (ii) and $\beta < \frac{\pi}{3}$ because $\lambda \leq \frac{\varrho}{2}$, which implies $\lambda_0 < \lambda$ as desired.

We now return to the radius of S, which is the distance between y and the closest point, w, of $\partial\mathbb{M}$. If w satisfies $\langle w, D_n(N(x))\rangle < \langle y, D_n(N(x))\rangle$, then d_x has positive slope at λ. Indeed, moving y a small distance along the distorted normal direction increases the radius. Since w must lie on the same side of H as x – for

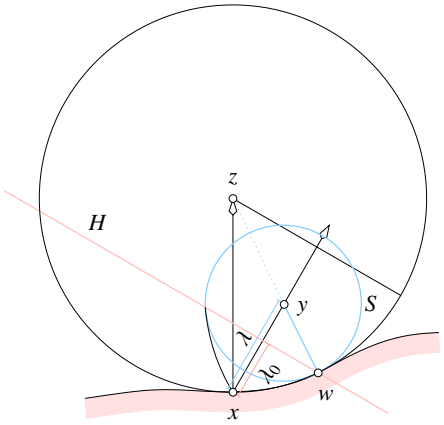

Figure 5: Illustration of the proof of Lemma 6. The circle centered at the point y on the distorted normal segment of x touches $\partial\mathbb{M}$ in the point w, which lies on or outside the circle centered at the point z on the normal segment of x.

else the sphere of radius ϱ that touches $\partial\mathbb{M}$ at w would enclose x – this inequality is satisfied as long as $\lambda_0 < \lambda$. Hence, d_x increases monotonically from 0 to $\frac{\varrho}{2}$. ◻

Since d_x is monotonic, it has an inverse, and we can write $L_x(d_x^{-1}(\theta))$ for the point at distance θ from $\partial\mathbb{M}$.

The segments cannot cross. Setting $\lambda = \frac{\varrho}{2}$, the lower bound in Lemma 6 implies that the distance between $y = L_x(\frac{\varrho}{2})$ and $\partial\mathbb{M}$ is at least $\frac{\varrho}{4}$. We use this simple fact to extend the *distorted normal segments* from $\mathbb{S}^{n-1}$ to $\partial\mathbb{M}$, defining

$$L_x = \{L_x(\lambda) \mid -\tfrac{\varrho}{2} \le \lambda \le \tfrac{\varrho}{2} \text{ and } |d_x(\lambda)| \le \tfrac{\varrho}{4}\} \tag{33}$$

for every $x \in \partial\mathbb{M}$. Recall the definition of the annulus, $\mathbb{A}_\theta = \partial\mathbb{M} + \theta\mathbb{B}^n$, set $\theta = \frac{\varrho}{4}$, and write $\mathbb{A} = \mathbb{A}_{\varrho/4}$. Since $\frac{\varrho}{4}$ is less than the reach, $\mathbb{A}$ has an inner and an outer boundary, $\partial_{\mathrm{i}}\mathbb{A}$ and $\partial_{\mathrm{o}}\mathbb{A}$, both diffeomorphic to $\partial\mathbb{M}$. By construction, L_x has one endpoint on the inner and the other endpoint on the outer boundary, for each $x \in \partial\mathbb{M}$. Since the distorted normal segments do not leave gaps, we have $\mathbb{A} = \bigcup_{x\in\partial\mathbb{M}} L_x$. We prove that this is a partition.

Lemma 7 *Let $\mathbb{M}$ be a solid body in $\mathbb{R}^n$, with* $\mathrm{reach}(\partial\mathbb{M}) \ge 2t\sqrt{n}$. *Then $L_x \cap L_y = \emptyset$ for all $x \neq y$ in $\partial\mathbb{M}$.*

Proof. In contrast to the parallel Lemma 3, the difficult part of this proof is to establish that the segments are pairwise disjoint. We do this in two steps, first considering *near* segments L_x, L_y defined by $\|x - y\| < \varepsilon_0$, for some small but positive constant ε_0, and second considering *far* segments defined by $\|x - y\| \ge \varepsilon_0$. Specifically, we first prove that near segments are necessarily disjoint, and we second show that if there are far segments that have a non-empty intersection, then there are also near segments that have a non-empty intersection.

For the first step, we focus on the inner boundary of $\mathbb{A}$, noting that the argument for the outer boundary is symmetric. Taking inward directed distorted normals, we map each point $x \in \partial\mathbb{M}$ to the point $L_x(d_x^{-1}(-\frac{\varrho}{4}))$ on $\partial_{\mathrm{i}}\mathbb{A}$. Consider a locally geodesic curve $\xi\colon \mathbb{R} \to \partial\mathbb{M}$ with $x = \xi(0)$ and velocity vector $\vec{x} = \dot{\xi}(0)$ at x. Correspondingly, we get a curve $\psi\colon \mathbb{R} \to \partial_{\mathrm{i}}\mathbb{A}$ with $q = \psi(0)$ and velocity vector $\vec{q} = \dot{\psi}(0)$ at q. Let H be the $(n-1)$-plane that passes through x and q such that $\vec{x}$ is normal to the $(n-2)$-plane in which $H - x$ intersects the tangent space of $\partial\mathbb{M}$ at x. It contains the line segment with endpoints x and q, and we call the open half-space that contains $x + \vec{x}$ the *positive side* of H. A sufficiently small motion along its curve moves x into the positive side of H. By Lemma 2 (ii), the angle between $\vec{x}$ and H is at least $60°$, and by combining Lemmas 4 and 5, we note that the angle between $\vec{x}$ and $\vec{q}$ is at most $\eta_1 + \eta_2 = 31.281\ldots° < 60°$. This implies that a small motion along its curve moves q into the positive side of H as well. We get the positive constant, $\varepsilon_0 < \mathrm{reach}(\partial\mathbb{M})$, because $\partial\mathbb{M}$ is compact and its curvature is bounded.

To prepare the second step, we let $\mathbb{X} \subseteq \partial\mathbb{M} \times \partial\mathbb{M}$ be the set of pairs (x, y) such that $L_x \cap L_y \neq \emptyset$. Eventually, we will establish $\mathbb{X} = \emptyset$, but for now we have a more modest goal, namely to show that $\mathbb{X}$ is compact. It is bounded since $\partial\mathbb{M}$ is bounded, so it remains to show that $\mathbb{X}$ is closed or, equivalently, that the limit of every Cauchy sequence in $\mathbb{X}$ belongs to $\mathbb{X}$ as well. To derive a contradiction, let $(x_1, y_1), (x_2, y_2), \ldots$ be a Cauchy sequence for limit (x, y), and suppose that $(x, y) \notin \mathbb{X}$. In other words, $L_x \cap L_y = \emptyset$. Because the segments are bounded and closed in $\mathbb{R}^n$, there is a threshold $\delta > 0$ such that the line segments remain disjoint even after thickening: $(L_x + \delta\mathbb{B}^n) \cap (L_y + \delta\mathbb{B}^n) = \emptyset$. By definition of Cauchy sequence and because the distorted normal segments of arbitrarily close points are arbitrarily close, there is a sufficiently large index j such that $L_{x_j} \subseteq L_x + \delta\mathbb{B}^n$ and $L_{y_j} \subseteq L_y + \delta\mathbb{B}^n$. But then $L_{x_j} \cap L_{y_j} = \emptyset$ and $(x_j, y_j) \notin \mathbb{X}$, which contradicts the assumption that $(x, y) \notin X$. Hence, $\mathbb{X}$ is compact, as desired.

In the second step, we suppose there are points x, y in $\partial\mathbb{M}$ whose distorted normal segments have a non-empty intersection. Hence $\|x - y\| \geq \varepsilon_0$, and because each distorted normal segment forms an angle at least $\frac{\pi}{3}$ with $\partial\mathbb{M}$, the distance of $z = L_x \cap L_y$ from $\partial\mathbb{M}$ is larger than a positive constant times ε_0. Using compactness of $\mathbb{X}$, the minimum distance of an intersection point between segments from $\partial\mathbb{M}$ exists, and we denote it as θ_0. Suppose now that the distance of z from $\partial\mathbb{M}$ is θ_0. Choose a positive radius $r < \frac{\varepsilon_0}{2}$ and let $S = S_r(x)$ be the set of points of $\partial\mathbb{M}$ at distance r from x. Because the radius is smaller than the reach, S is a topological $(n-2)$-sphere. Importantly, it separates x inside the sphere from y outside the sphere. Each point of S lies on a distorted normal segment, so we can transport S by moving the points along their segments, always making sure that the distance to $\partial\mathbb{M}$ is the same for all points. Since $r < \frac{\varepsilon_0}{2}$, these segments neither intersect L_x nor each other, which implies that the $(n-2)$-sphere at distance θ from $\partial\mathbb{M}$ encloses $L_x(d_x^{-1}(\theta)) \in \partial_{\mathrm{i}}\mathbb{A}_\theta$ for every $0 \leq \theta \leq \frac{\varrho}{4}$. But $L_x(d_x^{-1}(\theta_0)) = L_y(d_y^{-1}(\theta_0))$, so at least one of the segments intersects L_y. Because of the monotonicity of the signed distance function from $\partial\mathbb{M}$ along L_y, the intersection happens at a distance

less than θ_0 from $\partial\mathbb{M}$. But this is impossible by definition of θ_0, which provides the desired contradiction. ◻

The fibers cannot split. We have almost all ingredients ready to conclude that the distorted normal segments give a fibration of the symmetric difference. To construct it, we set

$$F_x = L_x \cap [(\mathbb{M} \setminus \mathbb{M}_t) \cup (\mathbb{M}_t \setminus \mathbb{M})] \tag{34}$$

for each $x \in \partial\mathbb{M}$, calling it the *fiber* at x. By construction, one endpoint of F_x lies on $\partial\mathbb{M}$ and the other on $\partial\mathbb{M}_t$. It is however possible that F_x is empty, namely iff $x \in \partial\mathbb{M} \cap \partial\mathbb{M}_t$, or that F_x meets $\partial\mathbb{M}_t$ in an interval rather than a point, namely only if L_x is normal to at least one coordinate axis. We will prove shortly that this exhausts all cases. In particular, it is not possible that F_x consists of two or more components.

Lemma 8 *Let $\partial\mathbb{M}$ be a smoothly embedded $(n-1)$-manifold in $\mathbb{R}^n$, with $1/\mathrm{curv}(\partial\mathbb{M}) \geq 4tn$ and $\mathrm{reach}(\partial\mathbb{M}) \geq 2t\sqrt{n}$. For every point $x \in \partial\mathbb{M}$, the fiber F_x is either empty or connected.*

Proof. To derive a contradiction, we assume that there is a point $x \in \partial\mathbb{M}$ such that L_x crosses $\partial\mathbb{M}_t$ three or more times. Sorting the crossings from inside to outside, we get $x_1, x_2, x_3, \ldots$, alternating between leaving and entering $\mathbb{M}_t$. Suppose the situation is as in Figure 6 in which we enter $\mathbb{M}_t$ at x_2. Let v and w be the centers

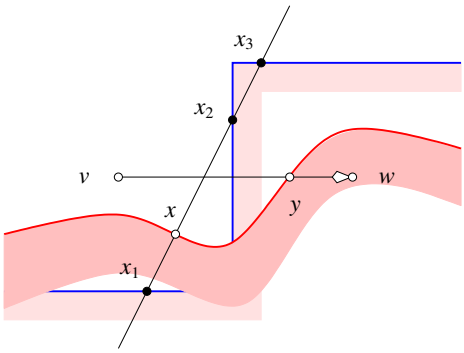

Figure 6: The distorted normal segment centered at $x \in \partial\mathbb{M}$ crosses the boundary of $\mathbb{M}_t$ at three points. The curvature of $\partial\mathbb{M}$ is exaggerated for better visibility.

of the n-cubes that share the face that contains x_2 in its interior, with $v \notin \mathbb{M}$ and $w \in \mathbb{M}$. By definition of digital approximation, the cube centered at v lies outside and the cube centered at w lies inside $\mathbb{M}_t$. Clearly, $\langle N(x), w - v\rangle > 0$, but to create this configuration, the two vectors have to be almost orthogonal. We show that they are sufficiently close to orthogonal such that $D_n(N(x))$ and $w - v$ are precisely orthogonal. To do so, we let y be the first point on the line segment from v to

w that belongs to $\partial\mathbb{M}$, and note that $\langle N(y), w - v\rangle \leq 0$. The Euclidean distance between the two points on the boundary of $\mathbb{M}$ is $\|x - y\| \leq \|x - x_2\| + \|x_2 - y\| \leq \frac{1}{2}t\sqrt{n} + \frac{1}{2}t\sqrt{n}$. The angle between the outward normals at the two points is at most

$$2 \arcsin \frac{\|x - y\|/2}{1/\mathrm{curv}(\partial\mathbb{M})} \leq 2 \arcsin \frac{\frac{1}{2}t\sqrt{n}}{4tn} \leq 2 \arcsin \tfrac{1}{8\sqrt{n}}. \tag{35}$$

Using $\arcsin x \leq 2x$, we conclude that the angle is at most $1/\sqrt{4n}$. According to Lemma 2 (i), this is the threshold below which the normal snaps to an orthogonal direction. Hence, $\langle D_n(N(x)), w - v\rangle = 0$, as desired. This contradicts that L_x intersects the symmetric difference in more than one component. ◻

7 Convergence for Solid Bodies

In this section, we prove that the digital algorithm implementing the modified first intrinsic volume is multigrid convergent for solid bodies. We begin with a proof that $\mathbb{M}$ and $\mathbb{M}_t$ have the same homotopy type.

Graded thickening. The goal is to shrink the fibers, but there is an obstacle, which we address first: some fibers are parallel and arbitrarily close to faces of $\mathbb{M}_t$ so shrinking leads to discontinuities. We therefore modify $\mathbb{M}_t$ without changing its homotopy type. Since $\mathbb{M}_t$ is closed, it is safe to thicken by a small amount, and to avoid faces parallel to fibers, we do this in a graded manner. Let $d_\pm : \mathbb{M}_t \to \mathbb{R}$ be the signed distance function from $\mathbb{M}$, mapping a point y to $d_\pm(y) = \pm \min_{x\in\partial\mathbb{M}} \|x - y\|$, in which the sign is positive outside and negative inside $\mathbb{M}$. Writing $c = \frac{1}{2}t\sqrt{n}$ for the half-length of a cube diagonal, we get $|d_\pm(x)| \leq c$ for all $y \in \partial\mathbb{M}_t$. To translate the signed distance into the grading, we choose a sufficiently small $\delta > 0$ and define $R(r) = -\frac{\delta}{c}r + 3\delta$, making sure that $\delta < c$ so that the slope is negative, with absolute value smaller than 1. The function is designed so that $2\delta \leq R(d_\pm(y)) \leq 4\delta$ for all $y \in \partial\mathbb{M}_t$, which is easy to check. To construct the *graded thickening* of $\mathbb{M}_t$, we first thicken by $R(d_\pm(y))$ and second shrink by δ:

$$\mathbb{M}_t^\delta = \mathbb{R}^n \setminus \left[\left(\mathbb{R}^n \setminus \bigcup_{x\in\mathbb{M}_t} [x + R(d_\pm(x)) \cdot \mathbb{B}^n]\right) + \delta \cdot \mathbb{B}^n\right]. \tag{36}$$

Because the slope of R is between -1 and 0, the thickening of interior points has no effect. It follows that $\mathbb{M}_t$ is thickened by an amount between 2δ and 4δ, so that shrinking by δ leaves a positive amount of thickening all around. After shrinking, the surface is without corners and creases, which is useful in forming a correspondence between $\mathbb{M}_t^\delta$ and $\mathbb{M}_t$. The following properties will be important.

Lemma 9 (Graded Thickening Lemma) *Let $\delta > 0$ be sufficiently small. Then $\mathbb{M}_t$ and $\mathbb{M}_t^\delta$ have the same homotopy type, and every distorted normal segment of $\partial\mathbb{M}$ intersects $\partial\mathbb{M}_t^\delta$ in a single point.*

Proof. Note that $\mathbb{M}_t \subseteq \mathbb{M}_t^\delta$. Because the normal directions at points of $\partial\mathbb{M}_t^\delta$ are well defined, every point $z \in \partial\mathbb{M}_t^\delta$ is the closest boundary point of a unique point $y \in \partial\mathbb{M}_t$. It is however possible that $y \in \partial\mathbb{M}_t$ has more than one closest point on $\partial\mathbb{M}_t^\delta$. We call the line segment from z to y a fiber, noting that the thus constructed fibers partition $\mathbb{M}_t^\delta \setminus \mathbb{M}_t$. Let $g\colon \mathbb{M}_t^\delta \to \mathbb{M}_t$ be defined by mapping every point on a fiber to its endpoint on $\partial\mathbb{M}_t$, and mapping every point of $\mathbb{M}_t$ to itself. It is continuous and homotopic to the identity on $\mathbb{M}_t^\delta$. This proves that $\mathbb{M}_t$ and $\mathbb{M}_t^\delta$ have the same homotopy type.

To prove the second claim, we note that already for $\partial\mathbb{M}_t$, the intersections with distorted normal segments are connected, namely points and intervals. The intervals arise because the distorted normal segments tend to align with the directions of the faces of $\mathbb{M}_t$. The graded thickening makes sure that such a segment intersects $\partial\mathbb{M}_t^\delta$ in a single point, and since we can make $\delta > 0$ arbitrarily small, we can avoid unwanted side-effects. ◻

The first property in the lemma certifies $\mathbb{M}_t^\delta$ as a feasible substitute for $\mathbb{M}_t$. The second property motivates us to define

$$F_x^\delta = L_x \cap [(\mathbb{M} \setminus \mathbb{M}_t^\delta) \cup (\mathbb{M}_t^\delta \setminus \mathbb{M})] \tag{37}$$

for every $x \in \partial\mathbb{M}$. Similar to the F_x, the F_x^δ partition the symmetric difference – this time between $\mathbb{M}$ and $\mathbb{M}_t^\delta$ – and every F_x^δ is either empty or a connected line segment. In addition, the F_x^δ define a homeomorphism between $\partial\mathbb{M}$ and $\partial\mathbb{M}_t^\delta$. This property is new and will be instrumental in what we will do next.

Homotopy equivalence. Using the new fibers, it is easy to establish that $\mathbb{M}$ and $\mathbb{M}_t^\delta$ have the same homotopy type. To explain this, we direct each fiber from outside to inside, and we distinguish between the fibers that partition $\mathbb{M} \setminus \mathbb{M}_t^\delta$ and the fibers that partition $\mathbb{M}_t^\delta \setminus \mathbb{M}$. We introduce $f\colon \mathbb{M} \to \mathbb{M}_t^\delta$ by mapping every point in $\mathbb{M} \setminus \mathbb{M}_t^\delta$ to the inner endpoint of the fiber that contains it, while mapping every point in $\mathbb{M} \cap \mathbb{M}_t^\delta$ to itself. Symmetrically, we introduce $h\colon \mathbb{M}_t^\delta \to \mathbb{M}$. Both maps are continuous, and it is not difficult to see that $h \circ f$ is homotopic to the identity on $\mathbb{M}$, and that $f \circ h$ is homotopic to the identity on $\mathbb{M}_t^\delta$. Indeed, we can retract the fibers in the two collections to create the two homotopies. This implies $\mathbb{M} \simeq \mathbb{M}_t^\delta$, and with $\mathbb{M}_t^\delta \simeq \mathbb{M}_t$ from the Graded Thickening Lemma we conclude that $\mathbb{M} \simeq \mathbb{M}_t$. While this is not the final goal of our investigations, we state it as one of our main results.

Theorem 3 (Homotopy Equivalence Theorem) *Let $\mathbb{M}$ be a solid body in $\mathbb{R}^n$, whose boundary is a smoothly embedded $(n-1)$-manifold in $\mathbb{R}^n$ with $1/\mathrm{curv}(\partial\mathbb{M}) \geq 4tn$ and $\mathrm{reach}(\partial\mathbb{M}) \geq 2t\sqrt{n}$. Then $\mathbb{M}$ and $\mathbb{M}_t$ have the same homotopy type.*

Interleaved filtrations. For the final step of the proof of convergence, we compare filtrations of sublevel and superlevel sets of height functions on $\mathbb{M}$, $\mathbb{M}_t$, $\mathbb{M}_t^\delta$.

For each direction $u \in \mathbb{S}^{n-1}$, we let $f_u \colon \mathbb{M} \to \mathbb{R}$, $g_u \colon \mathbb{M}_t \to \mathbb{R}$, $h_u \colon \mathbb{M}_t^\delta \to \mathbb{R}$ be the height functions in this direction, and fixing u, we write $\mathsf{F}_r = H(f_u^{-1}(-\infty, r])$, $\mathsf{G}_r = H(g_u^{-1}(-\infty, r])$ for the homology groups and $\mathsf{F}^r = H(\mathbb{M}, f_u^{-1}[r, \infty))$, $\mathsf{G}^r = H(\mathbb{M}, g_u^{-1}[r, \infty))$ for the relative homology groups. We collect the vector spaces in two towers, which we write one above the other:

$$\mathcal{F}\colon \quad 0 = \mathsf{F}_{-\infty} \to \ldots \to \mathsf{F}_r \to \ldots \to \mathsf{F}_\infty = \mathsf{F}^\infty \to \ldots \to \mathsf{F}^r \to \ldots \to \mathsf{F}^{-\infty} = 0, \tag{38}$$

$$\mathcal{G}\colon \quad 0 = \mathsf{G}_{-\infty} \to \ldots \to \mathsf{G}_r \to \ldots \to \mathsf{G}_\infty = \mathsf{G}^\infty \to \ldots \to \mathsf{G}^r \to \ldots \to \mathsf{G}^{-\infty} = 0. \tag{39}$$

To relate the towers, it would be convenient to establish inclusions between the sub- and superlevel sets, but they do not necessarily exist. The next best thing are continuous maps between the bodies that restrict to continuous maps between the sublevel and superlevel sets, and we have such maps $f \colon \mathbb{M} \to \mathbb{M}_t^\delta$, $g \colon \mathbb{M}_t^\delta \to \mathbb{M}_t$, $h \colon \mathbb{M}_t^\delta \to \mathbb{M}$ as introduced above. Before we continue, we note that the three maps move points along fibers of limited length. In particular the fibers for f, g, h have lengths at most $c, 3\delta\sqrt{n}, c + \delta$. Setting $c' = c + 3\delta\sqrt{n}$ and $c'' = c + \delta$ and restricting these functions to sublevel sets, we get

$$f_u^{-1}(-\infty, r] \xrightarrow{f} h_u^{-1}(-\infty, r + c] \xrightarrow{g} g_u^{-1}(-\infty, r + c'], \tag{40}$$

$$g_u^{-1}(-\infty, r] \hookrightarrow h_u^{-1}(-\infty, r] \quad \xrightarrow{h} f_u^{-1}(-\infty, r + c'']. \tag{41}$$

Noting that $c'' \leq c'$, this gives linear maps from F_r to $\mathsf{G}_{r+c'}$ and from G_r to $\mathsf{F}_{r+c'}$. Similarly we have maps from F^r to $\mathsf{G}^{r+c'}$ and from G_r to $\mathsf{F}_{r+c'}$. In other words, $\mathcal{F}$ and $\mathcal{G}$ are $(r + c')$-interleaved. The Stability Theorem of persistent homology implies the existence of a bijection $\beta \colon \mathsf{Dgm}(\mathcal{F}) \to \mathsf{Dgm}(\mathcal{G})$ with $\|A - \beta(A)\|_\infty \leq c'$ for all $A \in \mathsf{Dgm}(\mathcal{F})$. Each non-trivial pair in $\mathsf{Dgm}(\mathcal{G})$ corresponds to either a trivial or a non-trivial pair in $\mathsf{Dgm}(\mathcal{F})$. The number of pairs with persistence larger than $2c'$ in $\mathsf{Dgm}(\mathcal{G})$ is therefore bounded from above by the number of non-trivial pairs in $\mathsf{Dgm}(\mathcal{F})$, which is at most C. All other pairs have persistence at most $2c'$. Choosing $\varepsilon = 2c'$, the modified χ-moment ignores their contributions, which implies

$$|X(\mathcal{F}) - X(\mathcal{G}, 2c')| \leq 2c'C. \tag{42}$$

To get an upper bound on the difference between the intrinsic volumes, we still need to integrate over all $L \in \mathcal{L}_{n-1}^n$ and multiply with $c_{n-1,n} = \frac{nb_n}{b_{n-1}b_1}$; see (15) and (16). To state the final result, we choose $\delta > 0$ arbitrarily small so that $c' = c + 3\delta\sqrt{n}$ is arbitrarily close to $\frac{1}{2}t\sqrt{n}$.

Theorem 4 (Convergence Theorem for Solid Bodies) *Let $\mathbb{M}$ be a solid body in $\mathbb{R}^n$, with $1/\mathrm{curv}(\partial\mathbb{M}) \geq 4tn$, $\mathrm{reach}(\partial\mathbb{M}) \geq 2t\sqrt{n}$, and C an upper bound on the number of positive persistence birth-death pairs of any height function. Then the*

absolute difference between the first intrinsic volume of $\mathbb{M}$ *and the modified first intrinsic volume of* $\mathbb{M}_t$ *is*

$$|V_1(\mathbb{M}) - V_1(\mathbb{M}_t, t\sqrt{n})| \leq c_{n-1,n} t \sqrt{n} C. \tag{43}$$

The difference vanishes as t *goes to* 0*, which implies* $\lim_{t\to 0} V_1(\mathbb{M}_t, t\sqrt{n}) = V_1(\mathbb{M})$.

8 Discussion

We conclude our paper by explaining how the modified first intrinsic volume can be implemented, and by collecting open questions for future research. Before that, we put things into perspective by noting that our methods are not limited to digital approximations, which are considered mainly for their elementary description and relevance in applications.

Computation. As already mentioned in the introduction, it is possible to implement our algorithms. In this paragraph, we sketch the computation of the first intrinsic volume of a solid body $\mathbb{M}$ in $\mathbb{R}^n$ using a quasi-Monte Carlo method. First, we discretize the integral in (16) by sampling m uniformly distributed points on the unit sphere, $\mathbb{S}^{n-1}$, which we interpret as the normal directions of $(n-1)$-planes $L_i \in \mathcal{L}^n_{n-1}$. Second, we compute the modified χ-moments, $X(\mathcal{F}_i, t\sqrt{n})$, of the height functions of the resolution t digital approximations of $\mathbb{M}$ in these directions. Third, we approximate by averaging the m modified χ-moments. This approximation converges to $V_1(\mathbb{M}_t, t\sqrt{n})$, which in turn converges to the unmodified first intrinsic volume as we let t go to zero:

$$\frac{1}{m}\sum_{i=1}^{m} X(\mathcal{F}_i, t\sqrt{n}) \overset{m\to\infty}{\longrightarrow} V_1(\mathbb{M}_t, t\sqrt{n}) \overset{t\to 0}{\longrightarrow} V_1(\mathbb{M}). \tag{44}$$

In $n = 3$ dimensions, we can combine the Convergence Theorem for Solid Bodies with the convergence results for sampling directions in [9] to give bounds on the approximation error that only depend on the grid resolution, the complexity of the body, and the number of directions.

Open questions. The results in this paper open up a connection between the classic area of intrinsic volumes and the more recent area of persistent homology. There is much to be explored in terms of possible cross-fertilization. We mention two concrete questions that aim at generalizing or strengthening the results of this paper. Let $\mathbb{M}$ be a solid body in $\mathbb{R}^n$, ε_t a suitably chosen decreasing function that vanishes in the limit, and $n - k > 1$.

(1) Prove or disprove the convergence of $V^{\text{mot}}_{n-k}(\mathbb{M}_t, \varepsilon_t)$ to $V_{n-k}(\mathbb{M})$, as t goes to zero.

The first interesting case is the area measure for $n = 3$ and $n - k = 2$. In practical applications, the resolution to which ideal shapes can be approximated is limited.

(2) Extend the convergence results of this paper to stability results that hold for approximations at a fixed resolution.

To achieve stability, it will be necessary to replace the cutoff rule used in the definition of modified intrinsic volume in this paper by a softer transition, such as a standard ramp function, for example.

Acknowledgements

Both authors thank Anne Marie Svane for her comments on an early version of this paper. The second author wishes to thank Eva B. Vedel Jensen and Markus Kiderlen from Aarhus University for enlightening discussions and their kind hospitality during a visit of their department in 2014.

References

[1] U. Bauer and M. Lesnick. Induced matchings of barcodes and the algebraic stability of persistence. *In* "Proc. 30th Sympos. Comput. Geom., 2014", 355–364.

[2] P. Bendich, H. Edelsbrunner, D. Morozov and A. Patel. Homology and robustness of level and interlevel sets. *Homology, Homotopy, and Applications* **15** (2013), 51–72.

[3] T. Bonnesen and W. Fenchel. *Theorie der konvexen Körper.* Springer, Berlin, Germany, 1934.

[4] K. J. Böröczky, Jr, L. M. Hoffmann and D. Hug. Expectation of intrinsic volumes of random polytopes. *Period. Math. Hung.* **57** (2008), 143–164.

[5] F. Chazal, V. de Silva, M. Glisse and S. Oudot. The structure and stability of persistence modules. CGL Techn. Report, INRIA Saclay, France, 2012.

[6] D. Cohen-Steiner and H. Edelsbrunner. Inequalities for the curvature of curves and surfaces. *Found. Comput. Math.* **7** (2007), 391–404.

[7] D. Cohen-Steiner, H. Edelsbrunner and J. Harer. Stability of persistence diagrams. *Discrete Comput. Geom.* **37** (2007), 103–120.

[8] H. Edelsbrunner and J. L. Harer. *Computational Topology. An Introduction.* Amer. Math. Soc., Providence, Rhode Island, 2010.

[9] H. Edelsbrunner and F. Pausinger. Stable length estimates of tube-like shapes. *J. Math. Imaging Vision* **50** (2014), 164–177.

[10] H. Federer. *Geometric Measure Theory.* Springer, New York, New York, 1969.

[11] H. Hadwiger. Beweis eines Funktionalsatzes für konvexe Körper. *Abh. Math. Sem. Univ. Hamburg* **17** (1951), 11–23.

[12] H. Hadwiger. Additive Funktionale k-dimensionaler Eikörper I. *Arch. Math.* **3** (1952), 470–478.

[13] D. Hug. Random polytopes. In: *Stochastic Geometry, Spatial Statistics and Random Fields: Asymptotic Methods*, E. Spodarev (ed.), Lecture Notes Math. **2068**, Springer, Berlin, 2012, 205–238.

[14] M. Kiderlen. Introduction into integral geometry and stereology. In: *Stochastic Geometry, Spatial Statistics and Random Fields: Asymptotic Methods*, E. Spodarev (ed.), Lecture Notes Math. **2068**, Springer, Berlin, 2012, 21–47.

[15] R. Klette and A. Rosenfeld. *Digital Geometry.* Elsevier, San Francisco, California, 2004.

[16] D. Meschenmoser and E. Spodarev. On the computation of intrinsic volumes. Preprint 2010.

[17] J.-M. Morvan. *Generalized Curvatures.* Springer, Berlin, Germany, 2008.

[18] W. G. Nowak. Integer points in large bodies. In: *Topics in Mathematical Analysis and Applications*, T. M. Rassias and L. Toth (eds.), Springer Optimization and Its Applications **94**, Springer International, 2014, 583–599.

[19] J. Ohser and F. Mücklich. *Statistical Analysis of Microstructures.* John Wiley & Sons, Chichester, England, 2000.

[20] R. Schneider. *Convex Bodies: the Brunn-Minkowski Theory.* 2nd edition, Cambridge Univ. Press, Cambridge, England, 2014.

[21] R. Schneider and W. Weil. *Stochastic and Integral Geometry.* Springer, Heidelberg, Germany, 2008.

[22] A. M. Svane. On multigrid convergence of local algorithms for intrinsic volumes. *J. Math. Imaging Vision* **49** (2014), 148–172.

[23] H. Weyl. On the volume of tubes. *Am. J. Math.* **61** (1939), 461–472.